Volume 7 FEBRUARY, 1936 Number 2

PHYSICS

A Journal of General and Applied Physics

The Gassing of Lead Plate Storage Batteries During Charge and Discharge

W. B. PIETENPOL AND K. S. KELLER, *Department of Physics, University of Colorado*

(Received June 19, 1935)

The gases liberated from different types of lead plate storage batteries during varying conditions of charge and discharge have been collected and analyzed, and the corresponding changes in battery potential and specific gravity determined. A small amount of gas, mostly hydrogen, is given off by lead plate batteries during discharge and while idle, but a much larger amount of gassing takes place during the charging process, particularly near the end. In all cases of charging the gas consists almost entirely of hydrogen and oxygen, with a very small amount of acid vapor and water vapor. However, both the absolute and relative amounts of these gases depend upon the rate and method of charging. When high charging rates are used the gas is mostly hydrogen, while with low charging rates it is approximately half hydrogen and half oxygen. When batteries are charged steadily the ratio of hydrogen to oxygen is less than two to one, but when they are given rest periods during the charging process the ratio of hydrogen to oxygen is greater.

A STORAGE battery made with lead plates and an electrolyte of sulphuric acid gives off bubbles of gas during practically all of its life. This evolution of gas has been studied to a limited extent by different investigators during the past fifty years.

In 1883 Gladstone and Tribe[1] made some measurements on a battery of this kind. They placed lead plates covered with Pb_3O_4 in a dilute solution of sulphuric acid and passed an electric current through this solution for a number of hours. They found that hydrogen was evolved at the negative plate and oxygen at the positive plate. A certain amount of these gases produced by electrolytic action was absorbed by the plates, while the rest was released. The absolute amount absorbed per unit of time increased as the charging current was increased from one-half ampere to two amperes, but the percent absorbed decreased, thus producing a greater percent of wasted energy with the higher charging rate.

In 1912 Morse[2] found that a lead plate storage battery evolved a small amount of hydrogen during the first three-fourths of the charging process, but a considerable amount during the last one-fourth. He gives no information on oxygen evolved.

In 1928, Arendt[3] published results on gassing under various charging conditions. He used a modified constant current method and found that the amount of gas given off increased as the battery became more nearly charged. The composition of the gases evolved was variable depending upon the condition of the plates, but for marked gassing it was practically two parts of hydrogen to one of oxygen, as would be expected from electrolysis.

In 1930 Vinal[4] published results which were similar to those of Arendt. He states that during charge hydrogen is evolved at the negative plates and oxygen at the positive plates, and

[1] J. H. Gladstone and Alfred Tribe, *The Chemistry of the Secondary Batteries of Plante and Faure* (London, 1883), pp. 17 to 24.

[2] Harry W. Morse, *Storage Batteries* (New York, 1912), pp. 262 to 263.

[3] Morton Arendt, *Storage Batteries* (New York, 1928), pp. 156 to 157.

[4] George Wood Vinal, *Storage Batteries*, second edition (New York, 1930), pp. 243 to 244.

that the amount "depends on the current which is not absorbed by the battery." The gassing starts when the voltage at the terminal of the battery reaches about 2.3 volts per cell and increases as the voltage becomes larger. He found that it was not uncommon for one plate to begin gassing before the other, so during the early stages of charge the gases were not given off in the proportions of hydrogen and oxygen which form water. During the last part of the process, however, they were given off in the proportion of two parts of hydrogen to one of oxygen. He also states that gassing does not take place during discharge or when the battery is idle, except for the liberation of small amounts of hydrogen from the negative plates, which is due to local action.

While the results of these investigations agreed fairly well, no exact information regarding the quantity and quality of gases liberated from batteries could be found by the writers. In some preliminary experiments by one of the authors the gases were collected in a closed vessel and exploded by means of an electric discharge. Further attempts to unite the gases were made by means of electrically heated palladium asbestos. The results indicated that the relative percentages of hydrogen and oxygen evolved depended to a large degree upon the conditions which prevailed during the charging and discharging process. The following more exact and tedious analysis was therefore undertaken.

Method

Four different batteries were used. One was a new, standard, commercial type, 6-volt, 13-plate, 80-ampere-hour battery, hereafter referred to as Type A. Another was a new, standard, 6-volt, 13-plate, 86-ampere-hour battery of different manufacture and referred to as Type B. The third was an old 6-volt, 13-plate, Type A battery which had been used for a long time but still would give some service. The fourth was one which was built especially for this problem, and was constructed as follows:

A hard rubber case $7\frac{1}{8}$ inches long, $2\frac{5}{8}$ inches wide, and $7\frac{5}{8}$ inches high, ordinarily used as a jar for a two-cell radio battery, was used as the container. This case was originally divided into two equal compartments by a partition which ran from the top to the bottom, parallel to the width. The lower part of this partition was chiseled away to a height of one inch, so that the electrolyte in the cell could flow from one side to the other, or at least conduct current across. In one of the compartments was placed a single set of radio battery plates, used as positive plates, while on the other side was a set used as negative plates. Each set of plates was connected to its own conducting post extending through the top of the case and used as a terminal. The box was then filled with sulphuric acid solution having a specific gravity of 1.180, and the cell was charged and discharged as an ordinary battery.

The reason for building the battery in this particular form was that the gases given off by the two sets of plates could be collected separately, and thus more could be learned than from an ordinary battery.

In all but one of the runs the batteries were charged by the constant current method, with a 110-volt direct-current generator and putting the batteries in series with a high resistance. While this method of charging would not ordinarily be the most efficient one, it was believed to be the best for this problem because a record of ampere hours could be obtained more accurately by this method than by any other. Only a slight change of the resistance was necessary from time to time in order to keep the current constant. In one of the runs a modified constant potential method was used.

The batteries were all discharged through a suitable resistance and a record of ampere hours was again kept.

The gases evolved by the batteries were collected in the following manner: A hole was drilled in the battery cap of each cell and a glass delivery tube was sealed in the hole. The cap was then fitted with a rubber washer, screwed tightly to the cell, and sealed with a sealing compound. The delivery tube led to a graduated container full of water, and the battery gas was collected by displacing the water.

All volumes of gases were measured at room temperature and pressure. The temperature of the laboratory was very nearly constant, not varying more than two degrees from 24° centigrade. The pressure averaged about 630 mm of

mercury. All amounts of gases given for any battery are the gases evolved by a single cell of that battery.

Analysis of Gases

The apparatus and methods of gas analysis used were those suggested by Dennis and Nichols.[5] The gases were handled in a Hempel burette with water as the confining liquid.

First each sample was passed through a Hempel simple absorption pipette for solid and liquid reagents which contained a solution of one part of sodium hydroxide to two parts of water. This solution removed any water vapor, acid vapor, or colloidal particles of acid which were present. In the analyses reported later these substances are included under the heading of vapor.

Oxygen was determined by passing the gas through a solution of alkaline pyrogallol, potassium hydroxide being used as the alkali. Hydrogen was determined by mixing the sample with an excess of oxygen from air and passing this mixture through a tube full of palladium asbestos heated to 90°C. Two-thirds of the volume contraction which took place here was due to the hydrogen originally present.

These three determinations accounted for 99.3 percent of the samples analyzed, which was the limit of accuracy obtainable with the methods and apparatus used.

Results from New Type A Battery

Three runs were made with the new Type A battery. In the first two, conditions were maintained as nearly the same as possible in order to see whether repeating data could be obtained. The battery was charged at a 6-ampere rate at the start, and continued at that rate until the potential difference per cell while on the line had risen to 2.4 volts. At that point the charging rate was decreased to 3 amperes. Near the end of the charging part of the run the rate was again changed to 6 amperes for a short time.

Table I gives the data on the charging part of the first run. Potential differences are for one cell while on the line. Total gas is the number of cubic centimeters evolved up to the charge indicated under ampere hours. The percents of hydrogen, oxygen, and vapor given are for the gases evolved after the preceding analysis. Dashes in place of numbers indicate that for some unavoidable reason no reading was taken. Table II gives the results of the discharging part of Run I. The battery was discharged throughout at a 6-ampere rate. Potential differences are for one cell and were taken while the battery was delivering 6 amperes.

[5] L. M. Dennis and M. L. Nichols, *Gas Analysis*, revised edition (New York, 1929).

Table I. *Data on charging of new Type A battery.*

Ampere Hours	Specific Gravity	Potential Difference	Total Gas	Percent Hydrogen	Percent Oxygen	Percent Vapor
0	1147	1.96	0			
6	—	—	—			
12	1148	2.07	25			
18	1150	2.095	40			
24	1157	2.105	71			
		Idle for 10 Hours				
30	1175	2.13	86			
36	—	—	—			
42	1177	2.16	168			
48	1185	2.185	209			
54	1192	2.21	303			
60	1200	2.25	495	73.7	21.7	2.7
66	1215	2.31	888			
72	1233	2.365	1805	59.9	36.6	1.6
76	1250	2.4	2913	60.2	36.6	1.0
		Charging Rate Changed to 3 Amperes				
79	1253	2.35	3708	50.2	46.8	1.0
82	1265	2.365	4878	46.6	50.2	1.2
85	1280	2.375	6326	44.6	52.3	1.1
		Idle for 62 Hours				
86	1280	—	6750	38.7	57.4	1.8
		Charging Rate Changed to 6 Amperes				
87	1280	—	7430	57.7	38.9	1.4

Table II. *Data on discharging of new Type A battery.*

Ampere Hours	Specific Gravity	Potential Difference	Total Gas	Percent Hydrogen	Percent Oxygen	Percent Vapor
0	1275	—	0			
6	1265	2.04	40			
12	1252	2.03	81			
18	1248	2.015	105			
		Idle for 14.5 Hours				
24	1235	2.00	132			
30	1227	1.99	156	92.9	3.4	1.7
36	1215	1.98	179			
42	1207	1.965	199			
48	—	—	—			
54	1184	1.935	231			
60	1172	1.915	246			
66	1155	1.89	255			
72	1147	1.865	261	90.4	3.6	2.2

Final results for Run I, including both charge and discharge, are: Total gas evolved, 7691 cc; hydrogen 54.7 percent; oxygen, 41.9 percent; vapor, 1.4 percent.

Run II was handled very much like Run I except that the battery had a specific gravity of 1140 at the start instead of 1147, and so was given 92 ampere hours of charge instead of only 87. Final results of this run were: Total gas evolved, 9095 cc; hydrogen, 53.1 percent; oxygen 42.0 percent; vapor, 1.7 percent.

In both cases it was impossible to make a complete run without a rest period, so the battery was idle for a period of 10 to 14 hours near the start of the run, and for 62 to 65 hours near the end.

The corresponding percents in these two runs differed by an average of 0.7 percent. In both cases the ratio of hydrogen to oxygen was less than two to one.

In Run III an effort was made to charge by the constant potential method, but it was found to be impossible to keep the potential constant. At the beginning, with a potential difference of 2.3 volts per cell a current of 78 amperes was taken by the battery. During 75 minutes of charging the potential difference increased to 2.6 volts per cell in spite of all attempts to control it, with a decrease in current to 26 amperes. Results of this run were: Total gas evolved, 6238 cc; hydrogen, 59.1 percent; oxygen, 37.5 percent; vapor, 1.0 percent.

In this run the battery was idle for two periods, once for 16 hours and once for 4 hours. The ratio of hydrogen to oxygen again was less than two to one.

Results from Type B Battery

Four runs were made with the new Type B battery. In the first one, which will be called Run IV, conditions were kept as nearly like those of I and II as could be done in order that the batteries could be compared. Charging and discharging rates were the same, and the battery was idle for a period of 12 hours after it had received 36 ampere hours of charge.

Figs. 1 and 2 show information on this run, and are quite similar to graphs which were made of Runs I and II but are not printed in this report.

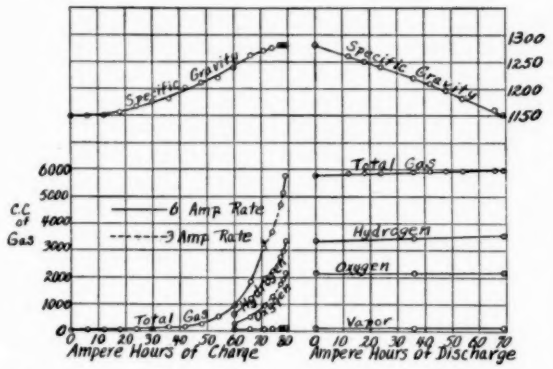

FIG. 1. Gases evolved during charge and discharge of Type B battery.

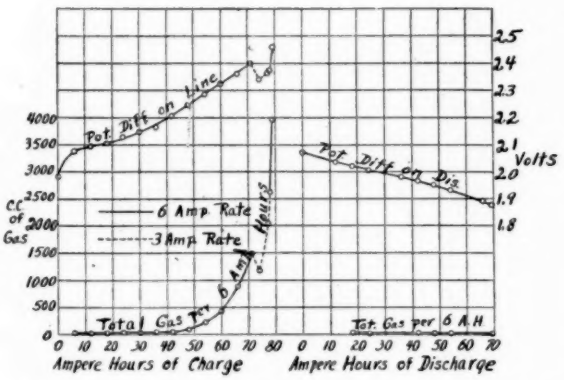

FIG. 2. Potential differences and rate of evolution of gases of Type B battery.

In Fig. 1 are shown specific gravity, total gas, hydrogen, oxygen and vapor. The values shown for the gases are the totals evolved up to that state of charge. In Fig. 2 are shown potential differences and total gas per 6-ampere hours. This last value is given for the reason that readings were usually taken each 6-ampere hours. When they were not taken at that interval, results were computed on that basis so they could be compared. Final results of Run IV are: Total gas evolved, 5992 cc; hydrogen, 59.1 percent; oxygen, 36.6 percent; vapor, 2.2 percent. The ratio of hydrogen to oxygen is less than two to one

In Run V the battery was charged but not discharged. It was given 69.5 ampere hours at a rate of 6 amperes, 3 ampere hours at 4 amperes, and 1.25 ampere hours at 3 amperes. The distinguishing feature of this run was that the battery was given 4 rest periods totalling 74 hours during the run. Results are: Total gas

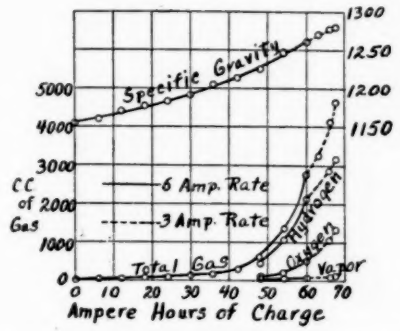

FIG. 3. Gases evolved of Type B battery when charged and rested alternately for 15-minute periods during charge.

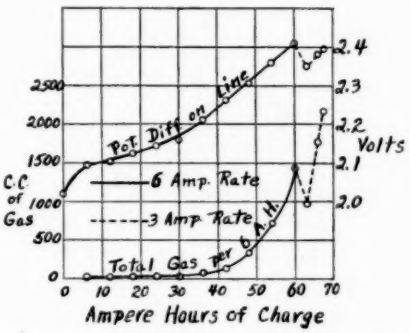

FIG. 4. Potential difference and total gas evolved for run shown in Fig. 3.

evolved, 5174 cc; hydrogen, 78.5 percent; oxygen, 17.6 percent; vapor, 2.0 percent. The ratio of hydrogen to oxygen is much more than two to one, being about four to one.

In Run VI the battery was charged for 15 minutes and rested 15 minutes alternately during all of the charge. The rate was 6 amperes until the potential difference on the line reached 2.4 volts per cell, at which time it was decreased to 3 amperes. No discharge was included in the run.

Figs. 3 and 4 give information on this run. Final results are: Total gas evolved, 4670 cc; hydrogen, 67.6 percent; oxygen, 28.3 percent; vapor, 2.3 percent. The ratio of hydrogen to oxygen is greater than two to one.

In Run VII the battery was charged, rested, and discharged for eight days at irregular intervals and at various rates. An attempt was made to subject it to the kind of treatment an automobile battery would receive under ordinary working conditions. Charging and discharging rates ranged from 2 to 10 amperes. Results for the eight days are: Total gas evolved, 8250 cc; hydrogen, 74.2 percent; oxygen, 22.7 percent; vapor, 1.4 percent. The ratio of hydrogen to oxygen is more than three to one.

Results from Old Type A Battery

The old used battery was charged in the same way as the new battery, that is, at 6 amperes to a potential difference of 2.4 volts and then at 3 amperes. No discharge test was made. Results of this run known as Run VIII, are: Total gas evolved 7411 cc; hydrogen, 53.8 percent; oxygen, 43.8 percent; vapor, 0.3 percent. The ratio of hydrogen to oxygen is less than two to one.

Results from Special Battery

The construction of this battery allowed the gases from two sets of plates to be collected separately, but it also made the capacity quite small. While the battery was being discharged after having received a full charge, its terminal potential difference decreased so rapidly that accurate measurements of capacity could not be obtained, but a rough estimate of two ampere hours was made.

In spite of this several interesting facts were obtained. While being charged, the negative plates gave off hydrogen and the positive plates oxygen. At the start of the charge only the negative plates gassed, while at the end both plates gassed, and hydrogen and oxygen were evolved in approximately the ratio of two to one, showing that electrolysis was taking place. The ratio of the total amount of hydrogen to the total amount of oxygen evolved during the whole of the charge was much greater than two to one.

During discharge only the negative plates gassed, and hydrogen was evolved. This was true if the battery was given a rest after being charged. If no rest was given, the positive plates gave off a small amount of oxygen for a short time. This was probably due to the occluded gases being released.

During a complete cycle of charge and discharge the negative plates gassed much more than the positive plates.

Discussion of Results

Most of the gassing done by a battery during a cycle of charge and discharge takes place dur-

ing the charge. In the cases studied about 97 percent of the total gas was evolved during the charge.

The gas given off by a battery during discharge is mostly hydrogen. The small amount of oxygen present was probably formed during the charge but was slow in being liberated.

Although statistics have not been given previously in this report, it was found during the study that the batteries gassed slightly when idle, practically all of the gas being hydrogen. The rate of gassing was higher for charged batteries than for discharged ones. The new batteries gassed from 3 cc per hour when discharged to 50 cc per hour when charged, while the old Type A battery gassed as much as 150 cc per hour when charged.

A summary of the results of the charging portions of all eight runs is shown in Table III.

The corresponding percents of gases given off by the new Type A and new Type B batteries, when handled in the same manner, agreed within six percent.

The gases evolved by the old Type A battery were quite similar to those given off by the new one, but as only one run was made with this battery the results were not as well established as some of the preceding ones.

In all cases it was found that the total amount of gas evolved per ampere hour by the batteries decreased as the charging rate was lowered. This was probably due to a certain limited amount and rate of chemical reaction being possible at the plates, and when the current was greater than that necessary for this amount the excess current was wasted in producing electrolysis.

Table IV, picked from four different runs, gives results which were typical of all runs. It shows the variation of the percents of gases given off with a change of the charging rate during a run.

TABLE III. *Summary of data of charging the various batteries.*

Run	Total Gas (cc)	Percent Hydrogen	Percent Oxygen	Percent Vapor
I	7430	53.4	43.2	1.4
II	8863	52.5	42.7	1.7
III	6238	59.1	37.5	1.0
IV	5787	58.2	37.6	2.2
V	5174	78.5	17.6	2.0
VI	4670	67.6	28.3	2.3
VII	8250	74.2	22.7	1.4
VIII	7411	53.8	43.8	0.3

TABLE IV. *Data showing the effect of charging rate.*

Run	Charging Rate (amperes)	Percent Hydrogen	Percent Oxygen	Percent Vapor
I	6	60.2	36.6	1.0
	3	46.6	50.2	1.2
II	6	56.2	39.4	1.4
	3	41.0	53.9	2.0
IV	6	61.8	34.9	1.1
	3	44.6	52.4	1.0
VI	6	74.0	22.2	2.1
	3	52.4	44.4	1.4

From this table it is seen that as the charging rate was decreased during a run the percent of hydrogen evolved decreased and the percent of oxygen increased. This may be due to the reaction at the positive plates being accelerated more than that at the negative plates by the higher potential difference across the cells during the higher charging rate. The reaction taking place at the negative plates during charge is: $PbSO_4+H_2O\rightarrow Pb+H_2SO_4$. That at the positive plates is first: $SO_4+H_2O\rightarrow H_2SO_4+O$; and then $PbSO_4+O+H_2O\rightarrow PbO_2+H_2SO_4$. The rate of the reaction at the negative plates probably does not change nearly as much with varying potential differences as does the second one at the positive plates. This is due to three reasons. First, the resistance of the PbO_2 is about 10,000 times as great as that of the Pb at the negative plates. This makes the reaction sluggish. Second, the Pb in the PbO_2 is in the tetravalent state, while the Pb at the negative plates is bivalent. Third, the mobility of the SO_4 ion is only about one-fifth that of the H_2 ion, so the ionic concentration at the positive plate is lower than at the negative plate.

At low charging rates, which result from low potentials, the percent of oxygen which reacts is small and a large percent is liberated as gas. At higher rates and potentials a larger percent reacts and a correspondingly smaller percent is liberated.

In the case of the Type B battery the effect of alternately charging and resting the battery was to produce a greater percent of hydrogen than was produced during a steady charge. This is believed to be due to the slow secondary reac-

tion at the positive plates being aided by the rests gained between charging periods.

There were two sources of error in the study. The larger of these was that occurring in the analyses of the gas. The average value of the sums of the percents reported was 97.9 percent. Several analyses were made quite carefully and averaged 99.3 percent. It was found that the time required to make the very careful analyses was much greater than that required to make those of 97.9 percent. The larger error was made by introducing small amounts of air at two steps in the analyses.

The second source of error was that due to a small amount of gas remaining above the electrolyte in the battery. This was made as small as possible by filling the cells as nearly full of distilled water as could be done without introducing new errors. The extent of this error was not greater than 80 cc in 6000 cc, or 1.3 percent, and was generally much less. Thus a total error of 3.4 percent was possible but not probable.

Spectral Emissivities, Resistivity, and Thermal Expansion of Tungsten-Molybdenum Alloys

P. N. BOSSART, *University of Pittsburgh*

(Received August 15, 1935)

The spectral emissivities of three different W-Mo alloys were found by direct measurement with an optical pyrometer to be from about 120 percent at 1300°K to 110 percent at 2200°K of the values calculated as a simple mixture of the constituents. In the case of one alloy this result was compared with a similarly determined ratio of measured to calculated resistivities. According to Drude's law, the square root of this resistivity ratio should be the corresponding emissivity ratio. It was found at temperatures 1300°K to 2100°K that the square root of the resistivity ratio was practically constant at 1.215, which checked approximately the emissivity ratio 1.19 at 1300°K only. The emissivities of W and Mo were measured. The resistivity-temperature, and thermal expansion-temperature relations are given for the alloy 46.5 percent atoms of W. The resistivity relation is compared with those of its constituents and discussed with reference to the theory of Bragg and Williams.

I. INTRODUCTION

THE spectral emissivities of tungsten[1–8] and molybdenum[2, 3, 9] have been carefully determined at incandescent temperatures, and this work extends the data for $\lambda=0.660\mu$ to include three different alloys of these two metals. The resistivity and thermal expansion are determined for one alloy. The work was done in the Research Laboratory of the Union Switch and Signal Company, but under the supervision of Dr. A. G. Worthing of the University.

II. METHOD

A. General

The method employed was that described by Worthing[6] for tungsten. A tubular filament with small holes pierced through the wall allowed a direct measure of spectral emissivity. The brightness of the filament surface was compared with that of a hole into the tubular center by means of a disappearing filament optical pyrometer.

B. Preparation of the filaments

The method used is that of Mr. W. P. Sykes, Metallurgist, Cleveland Wire Works.

1. *Paste.* The materials for the alloys were very finely divided tungsten and molybdenum powders obtained from The Cleveland Wire Works of the General Electric Company. A binder was made by dissolving 28 g of Parlodion (a very pure celluloid made by du Pont) in 400 cc of amyl acetate and 10 cc of castor oil. The powder obtained by a thorough dry mix of predetermined proportions by weight of the two metals was heated and stirred over a steam bath with about an equal weight of binder until thick enough to mold with the hands. The paste was then rolled and kneaded intermittently for several days, allowing it to stand in a thin sheet under a bell jar between workings.

When very stiff it was extruded through a die with an annular opening to form a paste tube 1 mm external and 0.5 mm internal diameter. (When the treatment of the filaments was complete, these diameters had shrunk to 0.72 mm and 0.34 mm.) Side holes 0.12 mm diameter were pierced with a fine wire, and filaments were shaped and clamped in U's, V's, or straight lengths while still plastic.

2. *Sintering.* The filaments were dried in the open for 24 hours, then overnight in an oven at 100°C. They were next sintered in an atmosphere of hydrogen using an electric resistor furnace common in the lamp industry. The temperature was raised gradually from 100°C to 300°C in four hours, then to 500°C during the next hour. By this time, any inflammable part of the binder had been driven off, and the temperature was

[1] Pirani, Physik. Zeits. **13**, 753 (1912).
[2] Mendenhall and Forsythe, Astrophys. J. **37**, 380 (1913).
[3] Burgess and Waltenberg, Bull. Bur. Standards **11**, 591 (1915).
[4] Pirani and Meyer, Electrot. u. Masch. **33**, 397, 414 (1915).
[5] Langmuir, Phys. Rev. **7**, 302 (1916).
[6] Worthing, Phys. Rev. **10**, 377 (1917).
[7] Henning and Heuse, Zeits. f. Physik **16**, 63 (1923).
[8] Lax and Pirani, Zeits. f. Physik **22**, 273 (1924).
[9] Worthing, Phys. Rev. **25**, 846 (1925).

then raised rapidly to 1600°C and held for one hour.

The filaments were next heated individually for several minutes under a bell jar in a stream of hydrogen by passing through them 90 to 95 percent of their fusing currents, corresponding[10] to temperatures 200 to 100° below the melting points. These currents varied from 44 amperes for Mo to 68 amperes for W. This treatment completed the alloying.

3. *Polishing.* The filaments were polished electrolytically in a bath of KOH. Solutions with specific gravities ranging from 1.01 to 1.20 were tried, and the best results were obtained with 1.03, using about four half-second flashes on a 230-volt d.c. circuit. The treating current density was about 30 amperes per sq. cm, just under the arcing density.

Further polishing was done by using 00, 000, and 0000 polishing papers (Manning Speed Grits) in turn.

C. Lamps

The filaments were mounted in 200-watt lamp bulbs. Some were evacuated, while others were filled through a rubber tube with commercial argon from burnt-out lamps. A few good gas-filled lamps were obtained, but the leak through the large rubber tube (4 cm I.D.) necessary for filling spoiled most of them.

The final lamp design, satisfactory for 50 amperes, used copper tube to lime glass seals, with about No. 12 B. & S. gauge copper lead-ins; and it had a permanently connected side tube of P_2O_5 (not in the furnace during baking out).

The lamps were exhausted at 400°C for two hours to a pressure of 10^{-5} mm of Hg, and the filaments were burned at about 2200°K for some minutes during exhaust.

A straight vertical filament with fine tungsten wires tied to it one inch apart, to serve as potential leads, was used for resistivity and expansion measurements.

D. Pyrometer calibration

Disappearing Filament Optical Pyrometer R2837 built at the University of Pittsburgh was calibrated with none, one, two, and three neutral tint absorbing screens, each of about 10 percent transmission. These screens were of Schott and Company's Jena Optical Glass, Type NG-3b, Melt No. 22,630, obtained from the Fish Schurman Corporation, New York City. This glass is more nearly neutral than any heretofore available. Its measured transmission varied from 0.107 to 0.111 in the range here of interest ($0.61\mu < \lambda < 0.73\mu$).

The monochromatic screen[11] was two thicknesses, each 5.7 mm thick, of Corning high transmission red glass whose limiting effective wave-length[12] varied from 0.662μ to 0.658μ over the range 1300°K to 2800°K.

Calibration was by extrapolation of the brightness curve in both directions using 1/2, 1/4, and 1/12 sector disks.[13, 14] Standardization was made from the University's standard lamp for the palladium point, taken as 1828.5°K; with C_2 of Wien's law as 1.432 cm °K.

E. Readings

The currents through the tubular filaments were held constant and the pyrometer currents were read with a Leeds and Northrup type K potentiometer modified[15] to a double potentiometer with one branch a deflection instrument. The resistivity was determined by drop of potential read on the same instrument. Expansion readings were made with two micrometer cathetometers, one focused on one tie wire and the second on the other tie wire.

III. Results

A. Emissivities

Fig. 1 shows the emissivities obtained for the pure metals and for the three alloys, 0.25, 0.625, and 0.875 W by weight as originally mixed. The sources of error pointed out by Worthing[6, 16] have been considered and none are believed to affect the brightnesses by more than 0.3 percent. Furthermore, the error due to neglecting the temperature difference between inner and outer filament surfaces, assumed to be of the order of

[10] Smithells, *Tungsten* (Chapman, 1926), p. 45.

[11] The glass was furnished by and effective wave-length determined by W. E. Forsythe.

[12] Forsythe, J. Opt. Soc. Am. **5**, 87 (1921).

[13] Mendenhall, Phys. Rev. **33**, 75 (1911).

[14] Forsythe, J. Opt. Soc. Am. **5**, 505 (1921).

[15] Worthing and Forsythe, J. Opt. Soc. Am. **10**, 601 (1925).

[16] Worthing, Phys. Rev. **4**, 163 (1914).

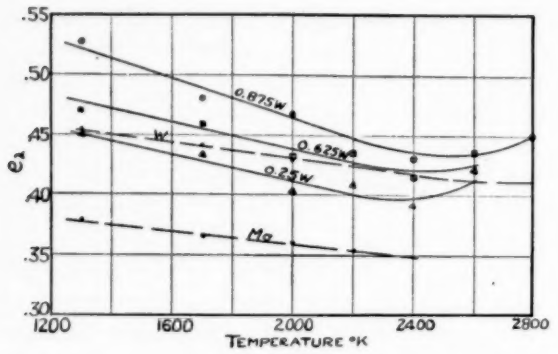

FIG. 1. Spectral emissivities for $\lambda=0.660\mu$ of W, Mo, and three alloys of the two, namely, 0.25W, 0.625W, and 0.875W by weight, as a function of temperature.

that found by Worthing for W, and the error due to finite size of hole, assuming the worst case of a matte interior surface, are of about the same size and in opposite directions. No corrections have been applied to these results. The values of e_λ are considered correct to ± 2 percent.

B. Variation with aging

The cause of the biggest variation in the measured emissivities was the change in the filament surfaces with continued burning of the lamps. So long as the temperature was held below the point where noticeable blackening of the bulb occurred on overnight burning, the emissivity of an alloy at a given temperature decreased to a steady value on prolonged burning. If heated to the point where sufficiently rapid evaporation took place, the emissivities for all temperatures increased, which probably means that Mo evaporated more rapidly than W and that the surface composition changed to an alloy richer in W which had a higher emissivity. Emissivities were determined after 24 hours or more of steady burning at temperatures from 2200°K to 2400°K and were checked after additional aging to make sure that they were not decreasing any more. The lowest values found were given most weight. All points plotted below 2400°K were the averages of two or more separate determinations.

The high temperature treatment (100° below MP) during manufacture may have changed the surface composition to one richer in W, but probably the polishing removed this surface layer, restoring one of the original composition. Geiss and Van Liempt[17] report that chemical analysis showed no noticeable change in composition of W–Mo alloys after similar heat treatment.

C. Emissivities of W and Mo

The results for W and Mo are shown compared with former work in Table I.

TABLE I. *Spectral emissivities of W and Mo.*

Observers	W T(°K)	W $\lambda(\mu)$	W e_λ	Mo T(°K)	Mo $\lambda(\mu)$	Mo e_λ
Pirani[1]	Independent	0.64	0.485			
Mendenhall and Forsythe[2]	1370	.658	.45	1300	0.658	0.44
	3170	.658	.66	2000	.658	.38
Burgess and Waltenberg[3]	2020	.65	.39	2300	.65	.43
Pirani and Meyer[4]	Independent	.532	.44			
Langmuir[5]	Independent	.664	.46			
Henning and Heuse[7]	2000	.647	.49			
Lax and Pirani[8]	2000	.650	.45			
Worthing[6, 9]	1300	.665	.456	1300	.665	.378
	1700	.665	.447	1700	.665	.364
	2000	.665	.439	2000	.665	.353
Bossart (this report)	1300	.661	.457	1300	.661	.378
	1700	.660	.441	1700	.660	.364
	2000	.659	.431	2000	.659	.360

For tungsten, the agreement with Mendenhall and Forsythe and with Langmuir at 1370°K only, and with Pirani and Meyer at 1500°K to 2000°K is good; with Lax and Pirani, fair; and with Worthing, good throughout; for molybdenum, the agreement with Mendenhall and Forsythe at 2000°K only is good; and with Worthing, good throughout.

D. Thermal expansion

The thermal expansion of the 62.5 percent W alloy may be expressed in the range 1100 to 2200°K by $\Delta L/L=3.5\times10^{-6}(t_{°C}-20)+1.6\times10^{-9}(t_{°C}-20)^2$. The coefficient of expansion at 1300°K is 6.7×10^{-6} per degree. For W[18] the value is 5.19×10^{-6} per degree at 1300°K and for Mo[19] is 6.05×10^{-6} per degree at 1300°K.

The coefficients of the linear terms in the expression for $\Delta L/L$ are in the case of W, the alloy, and Mo respectively 4.44, 3.5, and 5.00, all times 10^{-6}.

[17] Geiss and Van Liempt, Zeits. f. anorg. allgem. Chemie **128**, 355 (1923).
[18] Worthing, Phys. Rev. **10**, 638 (1917).
[19] Worthing, Phys. Rev. **28**, 190 (1926).

At 2000°K, $\Delta L/L$ from 293°K equals 0.0088, 0.0102, and 0.01154, respectively. It should be noted that while the expansion coefficient of the alloy at low temperatures is much less than that of its constituents, the expansion at 2000°K is approximately that calculated from its composition by volume.

E. Resistivity

In the range 1300°K to 2200°K, the resistivity of the 62.5 percent W alloy is 148±2 percent of the value calculated from the percent volume of the constituent metals, although at room temperature it is 226 percent as much as the calculated value. The temperature-resistivity relation may be expressed to one percent by

$$\rho_t = 12.72[1+2.69(t-t')10^{-3} + 0.27(t-t')^2 10^{-6}]\mu \text{ ohm cm},$$

$t = 293°\text{K}$ to $2200°\text{K}$,
$t' = 293°\text{K}$.

For $293 < t < 493°\text{K}$,

$$\rho_t = 12.72[1+2.75(t-t')10^{-3}].$$

Geiss and Van Liempt[17] report a minimum coefficient of 2.90×10^{-3} for 35 percent of Mo atoms in the W–Mo alloy series, as compared to 2.75×10^{-3} here for 53.5 percent atoms of Mo.

For Mo[20] the resistivity relation is

$$\rho_t = 5.14[1+4.791(t-t'')10^{-3} + 0.346(t-t'')^2 10^{-6}]\mu \text{ ohm cm}$$

where $273 < t < 2895°\text{K}$.

$$t'' = 273°\text{K}.$$

For W[18] the resistivity-temperature relation is best expressed by the equation

$$\frac{R}{R_0} = \left(\frac{T}{T_0}\right)^{\beta}$$

where T and T_0 lie between 1000 and 3200°K, and $\beta = 1.20$.

For Mo[19] the relation from 1000°K to 2895°K is the same except that $\beta = 1.145$.

The alloy measured satisfies this relation quite closely also, in the range 1600°K to 2200°K with $\beta = 1.17$ just about midway between the two values for its constituents; but below 1600°K, β is less, the value 1.05 holding well from 1000° to 1600°K. But below this it becomes less than 1 and is not constant.

[20] Worthing, Int. Crit. Tab. VI, p. 136.

F. Comparison with calculated values

Table II shows the relation between the values of e_λ measured and those calculated on a proportional basis taking into account the numbers of atoms of each metal present and the emissivities of the pure metals. The reason for this procedure is that the atomic volumes of W and Mo are very nearly the same; so if the alloy were a mechanical mixture, the percentage of atoms of W would be the same as the percentage of surface of W. The sum of the product for W of its fraction of surface times its emissivity and the corresponding product for Mo gave the calculated emissivity of the alloy. The measured values are from 10 percent at 2200°K to 20 percent at 1300°K higher than those calculated.

Drude's relation, $e_\lambda = 2(\rho/\lambda C)^{\frac{1}{2}}$, where ρ is the resistivity and C the velocity of light, fails to predict the decrease in emissivity as temperature increases, since it is known that the resistivities increase with temperature. This failure of the relation in the case of metals at visible wavelengths is well known. Nevertheless, one might say that if an alloy's emissivity is higher than calculated from its constituents, Drude's relation would lead one to expect the alloy's resistance should also be higher than that calculated from its constituents and in proportion to the square of the emissivity ratio.

TABLE II. *Comparison of calculated and measured emissivities of W–Mo alloys. e_λ for $\lambda = 0.660\mu$.*

Composition (percent wt. of W)	Composition (percent atoms of W)	Temp. (°K)	Emissivities Measured (percent)	Emissivities Calculated (percent)	Measured / Calculated
25	14.8	1300	45.0	39.0	1.15
		1700	43.0	37.5	1.14
		2000	41.0	36.5	1.12
		2200	40.0	36.0	1.11
62.5	46.5	1300	48.0	40.3	1.19
		1700	45.6	40.1	1.13
		2000	43.8	39.4	1.11
		2200	42.7	38.8	1.10
87.5	78.5	1300	52.6	43.9	1.20
		1700	49.1	42.8	1.15
		2000	47.5	42.1	1.13
		2200	45.7	41.6	1.10
Av. for all alloys		1300			1.18
		1700			1.14
		2000			1.12
		2200			1.10

TABLE III. *Comparison of calculated and measured emmissivities and resistivities for alloy of W and Mo, 62.5 percent W by weight and 46.5 percent W by percent atoms.*

TEMP. °K	ρ MEASURED (μ ohm cm)	ρ^* CALCULATED (μ ohm cm)	$\frac{\rho \text{ meas.}}{\rho \text{ cal.}}$	$\left(\frac{\rho \text{ meas.}}{\rho \text{ cal.}}\right)^{\frac{1}{2}}$	$\frac{\epsilon_\lambda \text{ meas.}}{\epsilon_\lambda \text{ calc. (from Table II)}}$
300	12.9	5.7	2.26	1.50	
500	19.8	10.8	1.84	1.35	
1300	50.6	33.7	1.50	1.22	1.19
1700	67.5	46.1	1.46	1.21	1.13
2000	81.6	55.7	1.46	1.21	1.11
2200	91.0	62.5	1.46	1.21	1.10

* Calculated on mixed crystal basis of percent of volumes (see F, paragraph 1).

However, as shown in Table III, at incandescent temperatures, the square roots of ratios of measured to calculated resistances do not fall as fast with temperature as the corresponding emissivity ratio; but stay almost constant at 121.5 percent$\pm$0.8 percent which is near the expected value at 1300°K only, where 119 percent is the emissivity ratio.

It would seem that at incandescent temperatures the alloy behaves much more like a mixture of its elements than at room temperature. β of the resistivity relation lies between the values of W and Mo, and the ratio of measured to calculated values is nearly constant, a condition not holding at room temperatures. In addition, the thermal expansion is intermediate to W and Mo at the higher temperatures but not at room temperature.

Bragg and Williams[21] explain the higher resistivity at higher temperatures of an alloy as compared to the resistivities of its constituents by thermal agitation producing a disorder in its structure where the atoms are not in the position of lowest potential energy, the disorder causing increased resistance just as well as the thermal agitation. This fits in with the 46 percent increase in resistance of the alloy over its constituents at 1600°K and above. These authors further explain the results of Kurnakow and Agnew[22] who examined the gold-copper alloy series by the idea that when the resistance falls sharply at a critical temperature, the atoms rapidly begin to find ordered positions in the crystal lattice, but that this proceeds at the lower temperatures at a slower and slower rate, so the positions of complete order at room temperature are not reached short of thousands of years and the state ordinarily obtained is that of equilibrium at a higher temperature. This accounts for the value at room temperature being greater than the value calculated from the constituents, but would seem to require a $\rho - t$ curve turning downward as the temperature falls, faster than the slope at high temperatures. The Au-Cu curves in the region 20°C to 600°C showed this effect. The curve here found shows no indication of a break downward at some critical temperature as the temperature falls, the resistivity value at room temperature being higher than the slope of the curve at high temperatures, if maintained, would give.

[21] Bragg and Williams, Proc. Roy. Soc. **A145**, 699 (1934).

[22] Kurnakow and Agnew, J. Inst. of Metals **46**, 481 (1931)

LETTERS TO THE EDITOR

This section will accept brief reports of new work of general interest to industrial physicists. The Editorial Board will not hold itself responsible for opinions expressed by the correspondents. Contributions to this section must reach the office of the Managing Editor not later than the twenty-fifth of the month preceding that of the issue in which the letter is to appear.

The Action of Alternating and Moving Magnetic Fields Upon Particles of Magnetic Substances

I have just come across Mr. C. W. Davis's paper on p. 184 of your June issue, in which reference is made to my explanation of the Mordey effect,[1] and to a paper by Dean, Gottschalk and Davis, published in 1934. The latter refer the Mordey effect rightly to permanent magnetism in the particles, but wrongly, as I believe my experiments demonstrate, to an orientation of the small permanent magnets by the first direction of the field, so that "in reversal they find themselves with their poles oriented against the field and are therefore repelled." Were this true, it would seem that they would be attracted by an equal amount on the next reversal of the field. It is quite easy to show by experiment that a short permanent magnet set with its axis in the direction of, but opposed to, a magnetic field does not experience any force of repulsion sufficient to overcome its friction upon a surface.

As I showed, a particle moves only when it is resting upon a surface loosely, with its magnetic axis at right angles to the alternating magnetic field, which furthermore must strike the surface at an angle other than 0° or 90°. The particle then moves towards the acute angle between field and surface. Mordey showed that a vertical a.c. bar magnet appears to repel magnetite particles when set *below* the surface, but he did not notice, or at any rate state, that it appears to attract them when set *above* the surface. As I showed, if the particles are stuck down with gum to the surface, and the latter is set on an arm of a torsion balance, no repulsive force whatever is observed. The mechanism of the action is convincingly shown by experimenting with a 2 or 3 mm piece of magnetized sewing needle resting upon a glass plate held in a clip. The needle only moves when its axis is set at right angles to the direction of the alternating field, and it is repelled or attracted as shown in Fig. 1. During one-half of a cycle the force on one pole is, say, obliquely downwards. The vertical component of this force presses the pole onto the plate, while its horizontal component, tending to move the pole towards the obtuse angle, is too weak to overcome friction. The other pole is, however, being simultaneously lifted off the plate by the vertical component, while the horizontal component drives the pole towards the acute angle. The needle thus makes a short step with one of its ends in the latter direction. When the field reverses, the other pole makes a step in the same direction. If a full length needle be magnetized and hung up by a thread attached to its middle point, and allowed to rest with one end upon a solid surface, the action of the alternating field upon a single pole can be demonstrated.

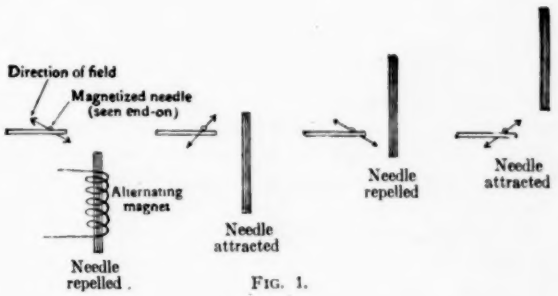

FIG. 1.

Similar considerations explain the action of a row of poles fed with polyphase current. The particles move against the field when the poles are below the surface, and with it when the poles are above the latter.

Mr. Davis says that I made no distinction between particles of low and high coercive force, but this distinction is obviously implied in the fact that I ascribe the effect to the permanent magnetism of the particles. Mordey already found that soft iron filings do not exhibit it. I must plead guilty, however, to having stated without explanation a striking effect observed with a rotating horseshoe magnet. If any kind of magnetic particles are sprinkled upon a surface set above the poles of such a magnet, they rush round at high speed in a direction opposite to the rotation of the magnet. If the magnet be inverted above the surface, they travel round in the same direction as the magnet. This effect is not due, I think, to the turning over pictured by Mr. Davis, which is of course observed with slow motion of magnet poles in a straight line, as figured by him in his paper. Since the Mordey effect with polyphase poles does not work on iron filings, turning over evidently fails at high speeds. In my experiment with the horseshoe magnet and iron filings, the filings rotate on the surface about a *vertical* axis at right angles to their length, since the magnetic field is rotating. Since, however, the field is somewhat oblique to the surface, one end of each filing is pressed more firmly on the surface than the other, and this is the inner end towards the axis of rotation when the magnet is above, and away from the axis when the magnet is below. Since the filing is spinning in the same sense as the magnet, its motion is thus explained.

Regarding spontaneous remagnetization, I mention in my paper that magnetite particles demagnetized by alternating current, and exhibiting practically no Mordey effect, regain their activity on keeping.

H. STAFFORD HATFIELD

University College,
London, England.
December 8, 1935.

[1] Hatfield, Proc. Phys. Soc. London **A46**, 604 (1934).

RHEOLOGY SECTION

The Motion of a Viscous Fluid Under a Surface Load. Part II

N. A. HASKELL, *Massachusetts Institute of Technology*

(Received December 14, 1935)

Following up previous work on the subsidence of a circular load on the surface of a highly viscous fluid, the same problem is treated for the case of a load in the form of an infinitely long strip with parallel sides. Simple expressions are derived for the limiting displacements as the system approaches hydrostatic equilibrium and for the form taken by the surface of the fluid at any time during the motion. Curves illustrating these quantities are plotted. It is pointed out that the subsidence of a load on the earth's surface having a span comparable to that of a continental ice sheet must produce appreciable flow at great depth. Using the previously derived figure for the mean viscosity of the earth it is found that with a load 2000 km wide equilibrium would be very nearly reached in about 18,000 years, and that loads of smaller span would require proportionately greater time to reach the same stage.

INTRODUCTION

IN a previous paper[1] the problem of the motion of a highly viscous fluid under a circular load applied on the free surface was treated with the particular object of determining the mean viscosity of the earth from the motion of the surface after the melting of one of the last continental ice sheets. Although it proved possible to derive a figure for the viscosity, the velocity distribution within the fluid could be given only in the form of definite integrals whose evaluation would require numerical integration. Since it is of some geological importance, in connection with the mechanism of isostatic adjustment, to have a roughly quantitative idea of the distribution of velocities, or at least of the final displacements, beneath a subsiding load, it was thought worth while to consider the same problem with a different load distribution which gives more tractable expressions for these quantities. Accordingly in the present paper we shall treat the case of an instantaneously applied load of constant thickness, having parallel sides, and whose length is sufficiently greater than the width so that it may be regarded as effectively infinite. As in I we suppose that the viscosity is so great that we may neglect the acceleration in the equations of motion in comparison with the terms expressing the viscous forces, and that the displacements remain small relative to the width of the load. We also assume the fluid to be incompressible.

[1] N. A. Haskell, Physics **6**, 265 (1935). Hereafter referred to as I.

1. SOLUTION IN TERMS OF DEFINITE INTEGRALS

We refer the equations of motion to a rectangular coordinate system having the plane $z=0$ in the undisturbed surface of the fluid, the positive z axis directed downward, and the y axis parallel to the length of the load, and let the width of the load be $2l$. Then V_y and $\partial/\partial y$ vanish and the equations of motion become

$$\partial^2 V_x/\partial x^2+\partial^2 V_x/\partial z^2=\partial\bar{p}/\eta\partial x, \qquad (1.11)$$

$$\partial^2 V_z/\partial x^2+\partial^2 V_z/\partial z^2=\partial\bar{p}/\eta dz, \qquad (1.12)$$

$$\partial V_x/\partial x+\partial V_z/\partial z=0, \qquad (1.13)$$

where $\bar{p}=p-\rho gz$.

Following the procedure used in I we let the equation of the free surface be given by $z=\zeta(x, t)$, and let the pressure exerted by the load be $\sigma(x, t)$. The boundary conditions are then

$$\bar{p}(x, o, t)+\rho g\zeta(x, t) -2\eta(\partial V_z/\partial z)(x, o, t)=\sigma(x, t) \qquad (1.21)$$

and

$$(\partial V_x/\partial z+\partial V_z/\partial x)_{z=0}=0. \qquad (1.22)$$

In the case with which we shall be concerned

$$\sigma(x,t)=\begin{cases}0;\ x>l \text{ or } <-l\\ 0;\ t\leq 0\\ \sigma=\text{const.};\ -l<x<l,\ t>0.\end{cases}\tag{1.23}$$

The method of solution is the same as that given in I and need not be repeated in detail. The only difference is that certain trigonometric functions replace the Bessel functions which occur there. The solutions are

$$V_x=(\sigma z/\pi\eta)\int_0^\infty e^{-\rho g t/2\eta\lambda-\lambda z}\sin\lambda l\sin\lambda x d\lambda/\lambda,\tag{1.31}$$

$$V_z=(\sigma/\pi\eta)\int_0^\infty e^{-\rho g t/2\eta\lambda-\lambda z}\sin\lambda l\cos\lambda x((1+\lambda z)/\lambda^2)d\lambda,\tag{1.32}$$

$$\bar{p}=(2\sigma/\pi)\int_0^\infty e^{-\rho g t/2\eta\lambda-\lambda z}\sin\lambda l\cos\lambda x d\lambda/\lambda,\tag{1.33}$$

$$\zeta=(2\sigma/\pi\rho g)\int_0^\infty(1-e^{-\rho g t/2\eta\lambda})\sin\lambda l\cos\lambda x d\lambda/\lambda.\tag{1.34}$$

To express these in dimensionless form set

$$\tau=\rho g l t/2\eta,\quad \alpha=x/l,\quad \beta=z/l,\quad \kappa=\lambda l,$$
$$v_x=2\eta V_x/\sigma l,\quad v_z=2\eta V_z/\sigma l,\quad \mu=\rho g\zeta/\sigma.$$

Then

$$v_x=(2\beta/\pi)\int_0^\infty e^{-\tau/\kappa-\kappa\beta}\sin\kappa\sin\kappa\alpha d\kappa/\kappa,\tag{1.41}$$

$$v_z=(2/\pi)\int_0^\infty e^{-\tau/\kappa-\kappa\beta}\sin\kappa\times\cos\kappa\alpha((1+\kappa\beta)/\kappa^2)d\kappa,\tag{1.42}$$

$$(\bar{p}/\sigma)=(2/\pi)\int_0^\infty e^{-\tau/\kappa-\kappa\beta}\sin\kappa\cos\kappa\alpha d\kappa/\kappa,\tag{1.43}$$

$$\mu=(2/\pi)\int_0^\infty(1-e^{-\tau/\kappa})\sin\kappa\cos\kappa\alpha d\kappa/\kappa.\tag{1.44}$$

The components of the displacement are given by

$$U_x=\int_0^t V_x dt=(\sigma/\rho g)\int_0^\tau v_x d\tau,$$

$$U_z=\int_0^t V_z dt=(\sigma/\rho g)\int_0^\tau v_z d\tau.$$

Hence, with $\xi=\rho g U/\sigma$,

$$\xi_x=(2\beta/\pi)\int_0^\tau(1-e^{-\tau/\kappa})e^{-\kappa\beta}\sin\kappa\sin\kappa\alpha d\kappa,\tag{1.51}$$

$$\xi_z=(2/\pi)\int_0^\tau(1-e^{-\tau/\kappa})e^{-\kappa\beta}\sin\kappa\cos\kappa\alpha(1+\kappa\beta)d\kappa/\kappa.\tag{1.52}$$

2. Evaluation of the Integrals

The integrals occurring in these expressions can be evaluated in terms of Bessel functions of the second kind for imaginary argument by the use of the inverted form of integral No. 927.0 in Campbell and Foster's tables.[2] With a slight change in their notation this integral may be written in the form

$$\int_0^\infty\exp(-\tau/\kappa-\kappa\beta-i\gamma\kappa)d\kappa/\kappa^{n+1}=2^{n+1}((\beta+i\gamma)/4\tau)^{n/2}K_n[(4\tau(\beta+i\gamma))^{\frac{1}{2}}].\tag{2.1}$$

By letting $\gamma=\alpha+1$ this becomes

$$\int_0^\infty e^{-\tau/\kappa-\kappa\beta}(\cos\kappa\alpha\cos\kappa-\sin\kappa\alpha\sin\kappa-i\{\sin\kappa\alpha\cos\kappa+\cos\kappa\alpha\sin\kappa\})d\kappa/\kappa^{n+1}$$
$$=2^{n+1}((\beta+i\alpha+i)/4\tau)^{n/2}K_n[(4\tau(\beta+i\alpha+i))^{\frac{1}{2}}]=N_n^{(+)}\tag{2.21}$$

[2] G. A. Campbell and R. M. Foster, "Fourier Integrals for Practical Applications," Bell Sys. Tech. Pub. Monograph B-584 (1931).

and by letting $\gamma=\alpha-1$

$$\int_0^\infty e^{-\tau/\kappa-\kappa\beta}(\cos\kappa\alpha\cos\kappa+\sin\kappa\alpha\sin\kappa-i\{\sin\kappa\alpha\cos\kappa-\cos\kappa\alpha\sin\kappa\})d\kappa/\kappa^{n+1}$$
$$=2^{n+1}((\beta+i\alpha-i)/4\tau)^{n/2}K_n[(4\tau(\beta+i\alpha-i))^{\frac{1}{2}}]=N_n^{(-)}. \quad (2.22)$$

(Note that $N_n^{(-)}$ is not the conjugate of $N_n^{(+)}$.) By adding (2.21) and (2.22) and equating real and imaginary parts we have the two real integrals

$$\int_0^\infty e^{-\tau/\kappa-\kappa\beta}\cos\kappa\alpha\cos\kappa d\kappa/\kappa^{n+1}$$
$$=\tfrac{1}{2}R[N_n^{(-)}+N_n^{(+)}] \quad (2.31)$$

and

$$\int_0^\infty e^{-\tau/\kappa-\kappa\beta}\sin\kappa\alpha\cos\kappa d\kappa/\kappa^{n+1}$$
$$=-\tfrac{1}{2}I[N_n^{(+)}+N_n^{(-)}]. \quad (2.32)$$

By subtracting we have

$$\int_0^\infty e^{-\tau/\kappa-\kappa\beta}\sin\kappa\alpha\sin\kappa d\kappa/\kappa^{n+1}$$
$$=\tfrac{1}{2}R[N_n^{(-)}-N_n^{(+)}], \quad (2.33)$$

$$\int_0^\infty e^{-\tau/\kappa-\kappa\beta}\cos\kappa\alpha\sin\kappa d\kappa/\kappa^{n+1}$$
$$=\tfrac{1}{2}I[N_n^{(-)}-N_n^{(+)}]. \quad (2.34)$$

Eqs. (1.41) to (1.44) may then be written in the form

$$v_x=(\beta/\pi)R[N_0^{(-)}-N_0^{(+)}], \quad (2.41)$$

$$v_z=(1/\pi)I[N_1^{(-)}-N_1^{(+)}]$$
$$+(\beta/\pi)I[N_0^{(-)}-N_0^{(+)}], \quad (2.42)$$

$$\bar{p}/\sigma=(1/\pi)I[N_0^{(-)}-N_0^{(+)}], \quad (2.43)$$

$$\mu=\mu_\infty-(\bar{p}/\sigma)_{\beta=0}=\mu_\infty$$
$$-(2/\pi)I[K_0\{(4i\tau(\alpha-1))^{\frac{1}{2}}\}$$
$$-K_0\{4i\tau(\alpha+1))^{\frac{1}{2}}\}], \quad (2.44)$$

where $\mu_\infty=\begin{cases}0; & x<-l \text{ or } x>l\\ 1; & -l<x<l.\end{cases}$

The displacements are

$$\xi_x=\xi_{x\infty}-(\beta/\pi)R[N_{-1}^{(-)}-N_{-1}^{(+)}], \quad (2.51)$$

$$\xi_z=\xi_{z\infty}-(1/\pi)I[N_0^{(-)}-N_0^{(+)}]$$
$$-(\beta/\pi)I[N_{-1}^{(-)}-N_{-1}^{(+)}], \quad (2.52)$$

where

$$\xi_{x\infty}=(2\beta/\pi)\int_0^\infty e^{-\kappa\beta}\sin\kappa\sin\kappa\alpha d\kappa, \quad (2.53)$$

$$\xi_{z\infty}=(2/\pi)\int_0^\infty e^{-\kappa\beta}\sin\kappa\cos\kappa\alpha(1+\kappa\beta)d\kappa/\kappa. \quad (2.54)$$

The integrals (2.53) and (2.54) cannot be evaluated directly by setting $\tau=0$ in (2.33) and (2.34), but may be treated separately as follows.

Integral No. 632.2 in Campbell and Foster's tables is

$$\int_{-\infty}^{+\infty}e^{-2\pi(\beta|f|+ixf-ifg)}df=\beta/\pi[\beta^2+(g-x)^2]. \quad (2.61)$$

Let $2\pi f=\kappa$, $g=\alpha$, $x=-1$. Then

$$\int_{-\infty}^{+\infty}e^{-|\kappa|\beta+i\kappa\alpha+i\kappa}d\kappa=2\beta/[\beta^2+(\alpha+1)^2].$$

By letting $x=+1$

$$\int_{-\infty}^{+\infty}e^{-|\kappa|\beta+i\kappa\alpha-i\kappa}d\kappa=2\beta/[\beta^2+(\alpha-1)^2].$$

By subtracting,

$$\int_{-\infty}^{+\infty}e^{-|\kappa|\beta+i\kappa\alpha}\sin\kappa d\kappa$$
$$=(\beta/i)[\{\beta^2+(\alpha+1)^2\}^{-1}-\{\beta^2+(\alpha-1)^2\}^{-1}]$$

or

$$\int_0^\infty e^{-\kappa\beta}\sin\kappa\sin\kappa\alpha d\kappa=(\beta/2)[\{\beta^2+(\alpha-1)^2\}^{-1}$$
$$-\{\beta^2+(\alpha+1)^2\}^{-1}]. \quad (2.62)$$

Hence

$$\xi_{z\infty}=4\alpha\beta^2/\pi\{\beta^2+(\alpha-1)^2\}\{\beta^2+(\alpha+1)^2\}. \quad (2.71)$$

Integrating (2.62) with respect to α from 0 to α gives

$$\int_0^\infty e^{-\kappa\rho}\sin\kappa\cos\kappa\alpha d\kappa/\kappa=\int_0^\infty e^{-\kappa\beta}\sin\kappa d\kappa/\kappa$$
$$-(\beta/2)\Big[\int_0^\alpha\{\beta^2+(\alpha-1)^2\}^{-1}d\alpha$$
$$-\int_0^\alpha\{\beta^2+(\alpha+1)^2\}^{-1}d\alpha\Big].$$

The first integral on the right is

$$\int_0^\infty e^{-\kappa\beta}\sin\kappa d\kappa/\kappa$$
$$=\int_0^\infty\int_\beta^\infty e^{-\kappa\beta}\sin\kappa d\beta d\kappa=\int_\beta^\infty\{\beta^2+1\}^{-1}d\beta$$
$$=\tan^{-1}(1/\beta).$$

The second and third are

$$\int_0^\alpha\{\beta^2+(\alpha-1)^2\}^{-1}d\alpha$$
$$=(1/\beta)[\tan^{-1}((\alpha-1)/\beta)+\tan^{-1}(1/\beta)]$$

and

$$\int_0^\alpha\{\beta^2+(\alpha+1)^2\}^{-1}d\alpha$$
$$=(1/\beta)[\tan^{-1}((\alpha+1)/\beta)-\tan^{-1}(1/\beta)].$$

Hence

$$\int^\infty e^{-\kappa\beta}\sin\kappa\cos\kappa\alpha d\kappa/\kappa$$
$$=\tfrac{1}{2}[\tan^{-1}((\alpha+1)/\beta)-\tan^{-1}((\alpha-1)/\beta)]$$
$$=\tfrac{1}{2}\tan^{-1}(2\beta/(\beta^2+\alpha^2-1)). \qquad (2.63)$$

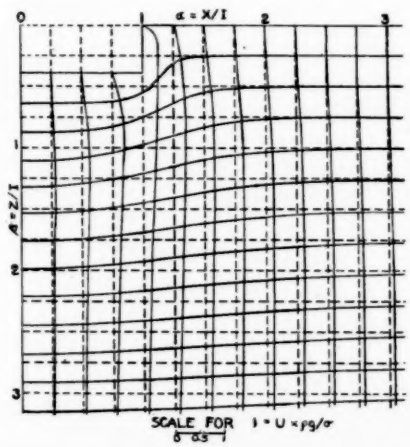

FIG. 1. Asymptotic displacements beneath a constant load.

For the second part of $\xi_{z\infty}$ the use of integral No. 632.11 of the tables gives

$$\int_0^\infty e^{-\kappa\rho}\sin\kappa\cos\kappa\alpha d\kappa$$
$$=(\beta^2-\alpha^2+1)/(\beta^2+(\alpha+1)^2)(\beta^2+(\alpha-1)^2). \quad (2.64)$$

Hence

$$\xi_{z\infty}=(1/\pi)[\tan^{-1}(2\beta/(\beta^2+\alpha^2-1)) \qquad (2.72)$$
$$+2\beta(\beta^2-\alpha^2+1)/(\beta^2+(\alpha+1)^2)(\beta^2+(\alpha-1)^2)].$$

It is easily shown that if $r=(\alpha^2+\beta^2)^{\frac{1}{2}}$ and $\theta=\tan^{-1}\alpha/\beta$, then for large values of r

$$\xi_{z\infty}\to\xi\sin\theta,\quad \xi_{z\infty}\to\xi\cos\theta,$$

where $\xi=(4/\pi)(\cos^2\theta)/r$.

3. Numerical Values

In Table I values of $\pi\xi_{z\infty}$ and $\pi\xi_{z\infty}$ computed from (2.71) and (2.72) are given for various values of α and β. In Fig. 1 these values are represented graphically, the solid lines giving the final positions of a set of rectangular lines whose initial positions are given by the dashed lines. Since the system is symmetrical in the zy plane, only one-half the field is represented.

To get a roughly quantitative idea of what this means in the case of a continental ice sheet on the earth let us suppose $l=10^8$ cm, take $\rho=5$ (i.e., a little less than the mean density of the earth), $g=10^3$, and let $\sigma=1.5\times10^8$ dynes cm^{-2} (approximately the pressure exerted by a sheet of ice 1500 m thick). Then $(x, z)=10^8$ (α, β) and $U=0.955\times10^4$ $(\pi\xi)$, hence with the scales used in Fig. 1 the displacement as shown is exaggerated by a factor of 1310. The great persistence with depth is noteworthy. In spite of the obviously great simplification of the problem we have treated as compared with the actual case, it seems clear that the isostatic compensation of such a load must be regarded as a distortion of the whole earth, as Daly[3] has contended, rather

[3] R. A. Daly, "Pleistocene Changes of Level," Am. J. Sci. 10, 281 (1925).

TABLE I. *Asymptotic values of the displacements* ($\times\pi$).

	β \ α	0.00	0.25	0.50	0.75	1.00	1.25	1.50	1.75	2.00	2.25	2.50	2.75	3.00
$\pi\xi_{x\infty}$	0.00	3.142	3.142	3.142	3.142	1.571	0.000	0.000	0.000	0.000	0.000	0.000	0.000	0.000
	0.25	3.121	3.115	3.040	2.854	1.570	.285	.063	.022	.009	.005	.003	.002	.001
	0.50	3.016	2.980	2.836	2.421	1.562	.700	.280	.123	.060	.024	.020	.014	.008
	0.75	2.815	2.768	2.557	2.149	1.541	.927	.504	.273	.154	.091	.058	.041	.026
	1.00	2.517	2.507	2.187	1.963	1.507	1.044	.672	.420	.264	.169	.112	.083	.054
	1.25	2.325	2.267	2.094	1.813	1.462	1.099	.782	.539	.368	.253	.177	.135	.091
	1.50	2.100	2.050	1.908	1.683	1.409	1.117	.850	.628	.457	.333	.243	.191	.133
	1.75	1.900	1.860	1.746	1.567	1.348	1.107	.887	.690	.538	.401	.304	.247	.178
	2.00	1.729	1.696	1.604	1.462	1.285	1.093	.903	.730	.581	.457	.359	.298	.222
	2.25	1.579	1.553	1.481	1.366	1.223	1.065	.905	.753	.618	.502	.404	.343	.263
	2.50	1.451	1.431	1.371	1.279	1.162	1.031	.896	.763	.642	.535	.442	.382	.299
	2.75	1.340	1.323	1.275	1.201	1.104	.995	.880	.765	.657	.558	.471	.413	.331
	3.00	1.244	1.230	1.191	1.129	1.050	.957	.859	.760	.664	.574	.492	.438	.358
$\pi\xi_{z\infty}$	0.00	0.000	0.000	0.000	0.000	1.000	0.000	0.000	0.000	0.000	0.000	0.000	0.000	0.000
	0.25	0.000	.062	.173	.480	.984	.488	.190	.092	.052	.033	.022	.016	.011
	0.50	0.000	.170	.400	.725	.941	.754	.461	.276	.173	.115	.080	.058	.043
	0.75	0.000	.235	.492	.745	.876	.800	.610	.431	.301	.214	.156	.117	.089
	1.00	0.000	.250	.492	.695	.800	.776	.662	.523	.400	.304	.232	.180	.141
	1.25	0.000	.235	.452	.624	.719	.726	.662	.564	.462	.371	.297	.238	.192
	1.50	0.000	.210	.400	.550	.640	.665	.635	.571	.492	.415	.345	.286	.236
	1.75	0.000	.183	.348	.480	.566	.603	.596	.556	.500	.437	.376	.321	.273
	2.00	0.000	.165	.301	.418	.500	.544	.551	.531	.492	.445	.394	.345	.300
	2.25	0.000	.136	.261	.365	.441	.488	.505	.499	.475	.440	.400	.358	.318
	2.50	0.000	.117	.226	.319	.390	.438	.461	.465	.452	.429	.397	.363	.329
	2.75	0.000	.102	.197	.280	.346	.393	.420	.431	.427	.412	.389	.362	.333
	3.00	0.000	.089	.173	.247	.308	.353	.382	.398	.400	.392	.376	.356	.332

than as a shallow horizontal flow beneath the crust. In this connection it may be of interest to compute the depth, z_0, below which one-half the total lateral displacement across a given vertical plane, $x=$const., takes place. The quantity of matter transported across a given vertical plane above an arbitrary depth z, per unit length of the load, is

$$\rho\int_0^z U_x dz=(\sigma l/g)\int_0^\beta \xi_x d\beta=\begin{cases}(\sigma l/\pi g)\{(\alpha+1)\tan^{-1}(\beta/(\alpha+1))-(\alpha-1)\tan^{-1}(\beta/(\alpha-1))\}; & \alpha>1\\ (\sigma l/\pi g)\{(\alpha+1)\tan^{-1}(\beta/(\alpha+1))-(1-\alpha)\tan^{-1}(\beta/(1-\alpha))\}; & \alpha<1.\end{cases} \tag{3.1}$$

The total quantity is

$$\rho\int_0^\infty U_x dz=\begin{cases}(\sigma l/g); & \alpha>1\\ (\sigma l\alpha/g); & \alpha<1.\end{cases} \tag{3.2}$$

The equation which determines $\beta_0=z_0/l$ is then

$$\begin{aligned}&(\alpha+1)\tan^{-1}(\beta_0/(\alpha+1))\\ &-(\alpha-1)\tan^{-1}(\beta_0/(\alpha-1))=(\pi/2); \quad \alpha>1;\\ &(\alpha+1)\tan^{-1}(\beta_0/(\alpha+1))\\ &-(1-\alpha)\tan^{-1}(\beta_0/(1-\alpha))=(\pi\alpha/2); \quad \alpha<1.\end{aligned} \tag{3.3}$$

TABLE II. *Depths below which one-half the total lateral displacement takes place.*

α	β_0	α	β_0
0.25	2.25	1.00	2.00
0.50	2.20	1.50	3.23
0.75	2.12	2.00	4.40

Table II gives the values of β_0 corresponding to various values of α.

The configuration of the surface at any time, given by (2.44), may be readily computed by expressing it in terms of the Hankel function $H_0^{(1)}(x\sqrt{i})$, where x is real, for which tables are available.[4] Let

$$x_1=\begin{cases}[4\tau(\alpha-1)]^{\frac{1}{2}}; & \alpha>1.\\ [4\tau(1-\alpha)]^{\frac{1}{2}}; & \alpha<1.\end{cases} \qquad x_2=[4\tau(\alpha+1)]^{\frac{1}{2}}.$$

Then

$$\mu=\begin{cases}-(2/\pi)I[K_0(x_1\sqrt{i})-K_0(x_2\sqrt{i})]; & \alpha>1\\ 1-(2/\pi)I[K_0(x_1\sqrt{-i})-K_0(x_2\sqrt{i})]; & \alpha<1.\end{cases} \tag{3.41}$$

By using the relationship $K_0(z)=(\pi i/2)H_0^{(1)}(iz)$, where z is any complex number, and taking care

[4] E. Jahnke and F. Emde, *Function Tables*, second edition (1933).

TABLE III. *Surface configuration at various times.*

α \ τ	$\frac{1}{16}$	$\frac{1}{8}$	$\frac{1}{4}$	$\frac{1}{2}$	1	3	10
0.00	0.145	0.236	0.370	0.545	0.742	0.977	1.007
0.25	.144	.234	.366	.538	.732	.967	1.008
0.50	.140	.227	.352	.515	.697	.929	1.007
0.75	.130	.213	.327	.471	.627	.837	.976
1.00	.118	.185	.273	.371	.457	.507	.500
1.25	.106	.155	.217	.269	.283	.177	.024
1.50	.094	.139	.186	.217	.204	.082	−.006
2.00	.082	.116	.145	.152	.118	.016	−.004
3.00	.067	.088	.099	.086	.045	−.005	+.002
4.00	.057	.070	.071	.052	.017	−.004	.000
5.00	.049	.058	.054	.032	.006	−.002	.000

to choose the proper root of $\sqrt{i}$ and $\sqrt{-i}$,[5] we have $I[K_0(x\sqrt{i})]=-(\pi/2)R[H_0^{(1)}(x\sqrt{i})]$ and $I[K_0(x\sqrt{-i})]=(\pi/2)R[H_0^{(1)}(x\sqrt{i})]$. Hence

$$\mu=\begin{cases}R[H_0^{(1)}[x_1\sqrt{i})-H_0^{(1)}(x_2\sqrt{i})]; & \alpha>1\\ 1-R[H_0^{(1)}(x_1\sqrt{i})+H_0^{(1)}(x_2\sqrt{i})]; & \alpha<1.\end{cases} \tag{3.42}$$

[5] $H_0^{(1)}$ vanishes at infinity if the imaginary part of the argument is positive, but becomes infinite if it is negative.

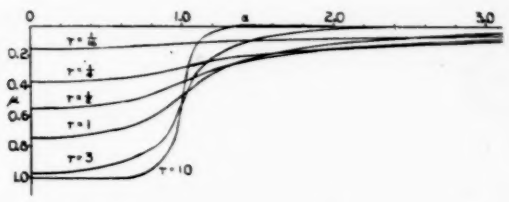

FIG. 2. Surface configuration at various times.

This function is tabulated in Table III and plotted in Fig. 2. If we use the value of $\eta/\rho=2.9\times10^{21}$ found in I and the l assumed above, then the unit of τ is approximately 1800 years. The figure for $\tau=10$ then shows that equilibrium would be very nearly reached in about 18,000 years. A load of smaller span would take a correspondingly greater time, e.g., one such as a river delta having $l=100$ km would require 180,000 years.

The Application of Chain Weight Loading to the Determination of Jell Strength*

IRVING J. SAXL, *Consulting Physicist, Providence*

(Received November 4, 1935)

In view of the importance of simple and precise methods for the determination of jelly strength, a new apparatus has been developed which permits the determination of jelly strength in terms of load *versus* compression. Chain weight loading is used for the gradual application or reduction of weight. The impression made in this manner within the gelatin specimen is compensated for by lifting it against the motion of a plunger with the aid of a calibrated micrometer screw. In this manner, it is possible to determine the load *versus* compression characteristics to better than three significant figures. The preparation of the sample has been standardized in such a manner that jelly strength determinations can be carried out at room temperature. Samples of load *versus* penetration diagrams are given. Also, the formation of hysteresis loops is described. The introduction of the term, jell factor, is suggested ($A = \frac{1}{2}$·breaking load·penetration (gram centimeters).

INTRODUCTION

THE jelly strength is considered one of the most important characteristics of gelatin. A number of methods and procedures have been developed therefore for the determination of the jelly strength. Among these, reference may be made to apparatus employing the shot loading principle such as the Bloom Test,[1] instruments for measuring the torsional elasticity such as the Sheppard Jelly Strength Testing Machine,[2] methods for testing the jelly strength that avoid the uncertainty of skin conditions that may form on the surface of test specimens such as the apparatus of Alexander,[3] devices using a penetrometer cone,[4] and others.

While these methods and apparatus provide means for the loading of test specimens, it appears difficult with any of the aforementioned types to determine exactly the gradual recovery of the test specimen after removal of the load. It also seemed that not only the final breaking point, such as indicated for instance by the well-known Lipowitz Jell Strength Apparatus, would be of interest but, particularly, the relation of load-*versus*-penetration over a reasonable range of observations before the final break occurs. Furthermore, fatigue effects, due to repeated loading and deloading, hysteresis characteristics, etc., seemed worthy of investigations. Last but not least, it is believed that a simplification of the experimental apparatus with a simultaneous increase in precision would be desirable. In view of the above, an instrument has been designed which will be described in the following.

THE INSTRUMENT

Inasmuch as the most commonly used test method is the "finger test," i.e., the subjective comparison of test samples by depressing them with the finger and comparing them against standardized test specimens, a method was developed that attempted to bring the results achieved by the "finger test" into objectively reproducible conditions of experimental technique. Such a method, to be suitable for use under most conditions, would necessitate compromises between demands of industrial practice and those of scientific precision. In the design of such an apparatus, a reasonably slow and continuous weight application, free from sudden jerks, is imperative. Moreover, it should be possible to add weight systematically as well as *reduce* it so as to be able to determine the recovery after the gelatin has been compressed.

For achieving the latter results, use is made of a chain weight loading device in this instrument. The gradually applied weight is transmitted to a plunger which produces the deformation of the

* Paper delivered before the meeting of the Society of Rheology, New York City, October 1935.

[1] F. L. DeBeaukelaer, J. R. Powell, E. F. Bahlmann, Industrial & Eng. Chem., p. 348, July 15 (1930).

[2] S. E. Sheppard, *Gelatin in Photography*. Vol. I. (Van Nostrand Co., 1923).

[3] Jerome Alexander, J. Soc. Chem. Ind. **24**, 459 (1908) also, *Glue and Gelatin*, p. 175 and U. S. Patent 882,731.

[4] J. M. Lutz, C. W. Culpepper, H. H. Moon and D. T. Meyers, Canning Age **14**, 404, 414, 428; (also in The Canner **77**, 11–14 (1933)).

gelatin. Compensation for this deformation can be made by lifting the gelatin sample against the deforming force with the aid of a micrometer screw. Accordingly, the penetration of the plunger into the jelly can be determined with exactness.

The problem of adding and deducting weight slowly and continuously can be solved simply by applying the chain weight principle, as used in chain vernier balances, to the gradual application of a load against the cohesion in a gelatin sample. The chain weight principle has found practical application before in the construction of chainomatic balances.[5] It has also been found useful in measuring the crinking of textile yarns[6] and in determining the load-*versus*-extension characteristics of various filamentous materials.[7, 8] It furthermore has been used for the compression of stationary gelatin samples.[9] In the construction described hereafter, chain weight loading has been applied in combination with an arrangement for measuring the depth of compression of the specimen with a precision of better than 0.05 mm. Moreover provision is made for lifting the one end of the chain to a constant height. This, in turn, makes possible to provide a direct calibration in grams upon the upright to which the other end of the chain is attached with the aid of a movable clamp.

The construction is simple and rugged. It permits not only constant and slow loading but also deloading without being bound to definite machine speeds such as given by a transfer of shot particles and similar weighting means (shot loading would not lend itself to weight removal). The application of the chain weight loading device furthermore permits waiting at critical points until equilibrium is reached during loading as well as deloading, and this at any point of the load-*versus*-compression characteristic. It also makes possible the study of the time factor as it refers to jelly deformation.

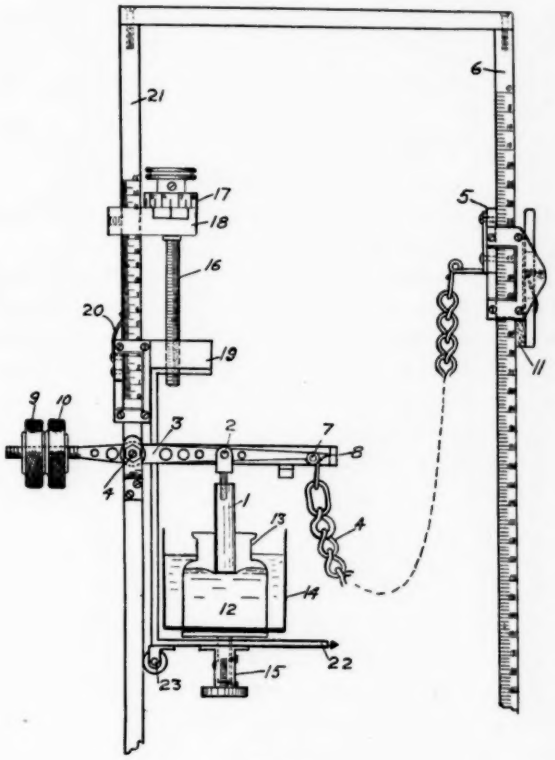

FIG. 1.

While the depth of deformation can be read precisely on a micrometer screw, the load can be read directly on a standing post which has been calibrated in grams. The construction of the apparatus is shown in Fig. 1. An aluminum plunger 1 with 1 cm² compressing surface hangs under its own weight free from an axle 2. This axle goes through a horizontal balance arm 3, the inertia of which has been reduced without impairing its stiffness by holes within the arm. The arm turns easily within precision conical bearings 4. On the right side of the arm there is attached a chain. (In actual practice a double chain is used.) The other end of the chain hangs on a movable support 5 that can slide up and down the graduated post 6. The holder 5 can be held at any height desired on the post 6 with the aid of the cork friction clamp 11.

When the holder 5 is all the way up so as to give the minimum possible weight application, then the pointer 7 of the arm 3 will indicate equilibrium by playing on a horizontal mark 8.

---

[5] Christian Becker, Met. and Chem. Eng. (4) **14**, 230 (1916).

[6] E. R. Schwarz and G. H. Hotte, "Optical Measurement of Yarn Waviness as Distinct from Crimp," Textile Research III **1**, 14 (1932).

[7] Irving J. Saxl, Some Dynamic Properties of Filamentous Materials, Textile Research **5**, 519–537 (1935).

[8] Irving J. Saxl, "A New Apparatus for Studying the Elastic Properties of Filamentous Materials," Rev. Sci. Inst. **6**, 409–412 (1935).

[9] S. E. Sheppard and S. S. Sweet, "A Preliminary Study of a Plunger Type Jelly Strength Tester," Ind. and Eng. Chem. **15**, 6, 571 (1923).

To make the original adjustment to this equilibrium, two brass weights 9 and 10 are movable at the left side of the pointer until equilibrium is reached at zero position of the pointer.

It will be readily understood that if the right side of the chain 4 is lowered, more weight will be applied to the left side of the chain thus loading the plunger 1 a definite amount.

The object which is compressed by the loaded plunger 1 is, in this instance, a standard test sample of gelatin 12 contained in the customary test bottles 13. The preparation of the jelly sample will be described in detail later on. To keep the temperature of the gelatin constant, the sample is held in a container 14 filled with water the temperature of which can be readily adjusted.

At zero position of the pointer 7, the gelatin sample 12 in the bottle 15 is raised with the aid of a lifting screw 15 until the plunger just touches the surface of the gelatin.

The actual lifting arrangement used in the investigation consists of a precision screw 16 with a micrometer head 17. By turning the screw which is held in bearings 18 a sled 19 is lifted or lowered. For achieving smooth motion, a spring 20 presses the sled 19 evenly onto the left post 21. Hanging from this sled 19 is a support 22 which moves smoothly upon the post 21 with the aid of the roll 23.

It will be understood that the jelly sample 12 will be deformed if the plunger 1 is pressed against the surface of the jelly 12. The depth of the compression can be ascertained directly by reading on the post 6 which is calibrated in grams. The exact amount of the depression can be measured by lifting the jelly sample 12 with the aid of the micrometer screw until the pointer 7 plays on the zero mark 8 again. Then the deformation that was made by a given load can be read on the micrometer screw to better than 0.05 mm.

It is, of course, possible to calibrate the instrument against standard samples of glues and thus to evaluate new glue samples to be tested quantitatively in terms of standard products.

While this apparatus measures jelly strength in the customary manner precisely, it should be mentioned that the same principle can be readily applied for testing the jelly strength in other ways, avoiding at the same time the uncertainty introduced by surface conditions of the jelly. For doing this, the same type of conical block described by Jerome Alexander[10] can be used. In this instance, a plunger that covers the upper surface of the conical jelly form completely may be used. Again, the deformation of the truncated cone can be measured in terms of the deforming load. However, by using the conical block, greater precautions have to be taken for the maintenance of temperature as the use of a constant temperature water bath, of course, is then not practical.

The Preparation of the Specimen

In the preparation of the samples, a deviation has been made from the customary practice of chilling the samples in an ice chest because it was felt that it was preferable to have such an arrangement that throughout can be worked at room temperature. For the purpose of getting reproducible results, the following routine has been adopted.

The gelatin samples are held at a temperature of 25°C during observation, with the aid of a water bath surrounding the sample. Inasmuch as 25°C is practically room temperature, small additions of either hot water, when the bath is too cold or small ice pieces, when it is too hot, are sufficient substantially to maintain the temperature of the testing samples. This is simpler than the constant temperature arrangements used in other gelometers. The gelometer sample is prepared in the following standard manner:

First 55.5 grams of gelatin are dissolved in 200 cc cold water. They are allowed to stand for 15 minutes, then held at 60°C for 20 minutes. One-tenth cm^3 cresylic acid is added as a preservative. Approximately 90 cm^3 of the samples are poured into the jell strength bottles and allowed to harden at 25° (for 18 hours) with the rubber cover closed. In this manner evaporation from the surface of the specimen is held at a minimum. If the samples are prepared in the afternoon, they are ready for use the next morning.

[10] Jerome Alexander, J. Soc. Chem. Ind. **27**, 459 (1908); also, U. S. Patent 882,731.

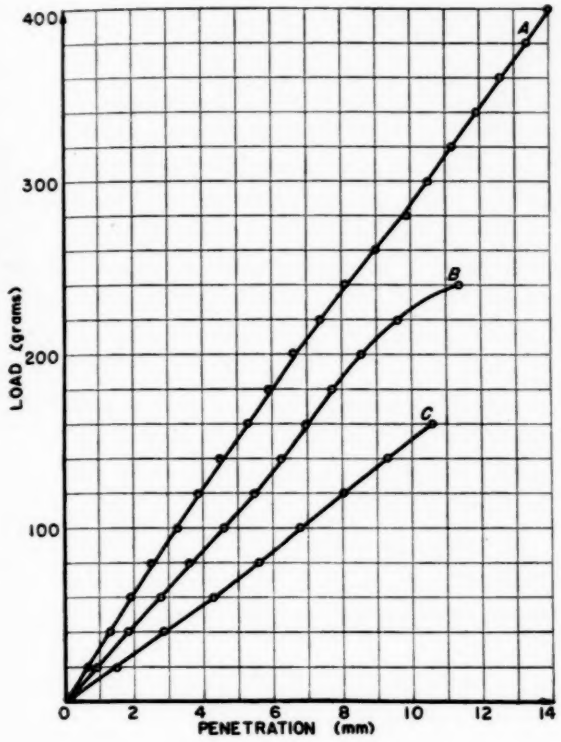

FIG. 2.

The sample is now inserted in the jelly tester within a water bath consisting of a beaker filled with water at 25°C. Readings are taken for each successive position of the load application at intervals of two minutes. Fig. 2 shows load-*versus*-penetration curves determined in this manner. Curves *A*, *B* and *C* represent different types of gelatin taken from samples of nationally known manufacturers.

It can be readily seen that the jell strength in curve *A* is higher than in *B* and that again, the jell strength of the *B* sample is higher than in *C*. These curves were continued until the gelatin ruptured. It can be seen that up to this point the relation of load-*versus*-penetration follows a linear law.

THE JELL FACTOR

In comparing gelatins, it is suggested to adopt a term which may designate the *jell factor*. This appears to be of importance in view of the fact that the slope of the load-*versus*-penetration curve *alone* is not indicative of the jell strength of a gelatin. Under actual conditions it sometimes happens that gelatins of a high slope of ascent of the load-*versus*-penetration curve break at a smaller depth of penetration than other gelatins with a lower angle of ascent.

While tests such as the Bloom Test give the total force necessary for a standard penetration (4 mm in the case of the Bloom Test), it appears to be a fairer basis of comparison to determine *the total work necessary before the final break in the jelly occurs.*

Inasmuch as the load-*versus*-penetration characteristic of gelatins is practically a straight line until the yield point, the jell factor should be determined in terms of the area of the triangle included between the load-*versus*-penetration curve and the abscissa. The area, *A*, then is

$A = \frac{1}{2}$. Breaking Load · Penetration (gram centimeters).

This result, multiplied by a numerical constant, *C*, can be compared with the expression for jelly strength suggested by Sheppard which is in terms of torsional elasticity of a jelly cast,[11] and is

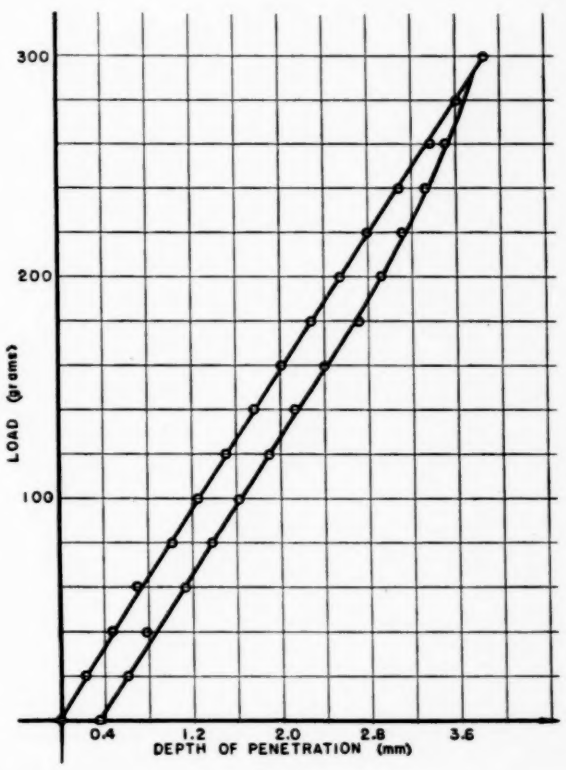

FIG. 3.

[11] S. E. Sheppard, *Gelatin in Photography* (D. Van Nostrand, 1923), p. 217.

proportionate to "proof resiliency." In the case of type *A* gelatin shown in Fig. 2, the jell factor would then be

$$A_A = 1/2 \cdot 400 \cdot 1.4 = 280 \text{ (g cm)}.$$

In the case of type *C* gelatin, the jell factor would be less, *viz.*,

$$A_C = 1/2 \cdot 160 \cdot 1.06 = 84 \text{ (g cm)}.$$

Hysteresis

As previously indicated, the apparatus described above lends itself not only to measuring the deformation of a gelatin under an applied force but it also permits the determination of the partial recovery of the gelatin while the load is removed gradually. Fig. 3 shows diagrammatically the conditions taking place. It will be understood that the area circumscribed by the hysteresis loop is indicative of the internal distributing forces which counteract the recovery of the gelatin.

While during the loading of the gelatin the load-*versus*-penetration curves practically follow a linear law, at the beginning of the deloading of the gelatin this relation no longer follows a straight line characteristic. However, after some recovery, a straight line relationship holds true for further weight reduction, the lower part of the descending characteristic being practically parallel to the ascending portion.

The ability to recover elastically, without excessive permanent deformation is a valuable characteristic for gelatins that have to recover from repeated loading and are subjected to mechanical fatiguing. Inasmuch as the above apparatus lends itself readily to the determination of hysteresis characteristics, this important property of gelatins can be investigated at the same time.

Rheological Properties of Asphalts

III. A Viscosity Index[1, 5]

R. N. TRAXLER AND H. E. SCHWEYER, *The Barber Asphalt Company, Maurer, N. J.*

(Received October 31, 1935)

A review is given of the work which has been done on the temperature-viscosity relations of bituminous materials and it is pointed out that the methods commonly used for evaluating the changes of consistency with temperature are empirical and unsatisfactory. Viscosity measurements at temperatures ranging from 15° to 35°C have been made on fourteen asphalts of paving consistency by means of the alternating stress method described by Bingham and Stephens. It has been found that for these asphalts and temperatures a plot of the logarithm of viscosity against temperature gives essentially a straight line. An asphalt viscosity index is established which is defined by the relationship:

$$\text{A.V.I.} = 100(10^a - 1),$$

where "a" is the slope of the log viscosity *versus* temperature plot. To obtain numerical values for the A.V.I. it is only necessary to determine experimentally the viscosity at two temperatures (in the range where the straight line relation holds) and substitute in the expression:

$$\text{A.V.I.} = 100\left[\left(\frac{\eta_c}{\eta_d}\right)^{1/(t_c - t_d)} - 1\right],$$

where η_c and η_d are the viscosities (in poises) at t_c and t_d (°C), respectively. This gives the percentage decrease in viscosity of the asphalt for 1°C rise in temperature. The values obtained for the viscosity index for the asphalts studied varied from 19.2 for Venezuelan oil asphalt prepared in a batch steam still to 24.7 for a vacuum reduced Californian oil asphalt.

INTRODUCTION

THE susceptibility, that is, the change of viscosity with change in temperature, is recognized as an important characteristic of bituminous materials. The methods proposed for evaluating these temperature-viscosity relations have been based upon arbitrary tests wherein some function of absolute viscosity such as penetration, softening point or time of efflux at an elevated temperature was used. Although consistencies as measured by these various empirical methods are related to the viscosity, these relations are usually quite involved, as has been pointed out for penetration *versus* viscosity.[1]

The literature contains very few references to the temperature-viscosity relations of asphalt and when these relations have been studied no attempt has been made to utilize the data for the establishment of a susceptibility index. Most investigators have been more interested in obtaining the actual viscosities at various temperatures than in comparing rates of change of viscosity with temperature. Also, with few exceptions, straight line relationships between temperature and viscosity have not been obtained over a very wide temperature range.

Rodiger[2] made a study of the temperature-viscosity relations of asphalt and tar and of asphalt-tar mixtures over a temperature range of 25° to 109°C using a Tsuda capillary viscometer. He did not attempt to establish equations for the relationship.

Saal[3] gave an excellent review of the rheological properties of asphaltic bitumens and described a number of instruments which may be used to measure the flow properties of such materials. His own data gave curved lines for log viscosity *versus* temperature plots, and in order to obtain a straight line relationship he used the formula:

$$\log \log (V_K + 1) = m \log T + c, \qquad (1)$$

where V_K is kinematic viscosity in centistokes, T is absolute temperature (273+°C), and m and c are constants.

The American Society for Testing Materials[4] has proposed a similar equation for lubricating oils. This formula, which Saal admits may be criticized because of the double logarithm, has

[1] R. N. Traxler, C. U. Pittman and F. B. Burns, Physics **6**, 58 (1935).

[2] W. Rodiger, Kolloid Zeits. **66**, 351 (1934).

[3] R. N. J. Saal, Proc. World Petroleum Congress **2**, 515 (1933), London, England.

[4] Proc. Am. Soc. Testing Materials **32**, part I, 772 (1932).

been found not to hold over a wide range of temperature.[5]

Umstätter[6] studied the effect of temperature on the viscosity of asphalts, by means of a rotating cylinder viscometer, and obtained straight lines over the range 25° to 50°C by plotting the logarithm of viscosity against the reciprocal of the square of the absolute temperature, i.e.,

$$\log \eta = mT^{-2} + b, \qquad (2)$$

where η = viscosity in poises,

T = absolute temperature (273 + °C),

and m and b are constants.

This equation has been found to give a good approximation to a straight line when applied to data obtained in our laboratory for a number of different kinds of bitumen over a temperature range of 15° to 50°C. The relationship, also, holds fairly well for various asphalts over the range 80° to 200°C, but for any bitumen the value of m for the higher temperature range is different from that for the lower. Thus, in the region of 50° to 80°C the lines plotted for these asphalts using Eq. (2) meet at an angle, indicating a radical change in the characteristics of the bitumen. It is significant that the softening points of the asphalts lie between 50° and 80°C, further indicating some fundamental change in the structure of the bituminous system. This change in structure probably accounts for the difficulties encountered in obtaining a simple expression for temperature-viscosity relations over an extended temperature range.

Some researches concerning the viscosity of bitumens and their change of consistency with temperature have been reported by Hoepfner and Metzger,[7] and by Hoepfner.[8] They used graphical methods for determining an index which relates such physical characteristics as freezing point, dropping point (Ubbelohde), Ring and Ball and Kramer-Sarnow softening points to temperature. Their freezing point is based on an arbitrary penetration method.[9] Lenhard[10, 11] has presented data supporting the validity of the Hoepfner-Metzger index whereas Klinkmann[12] has written a critical review in which he indicated the weaknesses of the method. Because the Hoepfner-Metzger system uses special apparatus and arbitrary methods and expresses the results in units that have no definite meaning, the method merits little consideration.

Two indices that have been rather widely used to compare the susceptibility of asphalts on the basis of penetration are given below:

Susceptibility factor[13]

$$= \frac{\text{Pen. 115°F 50 g/5 sec.} - \text{Pen. 32°F 200 g/60 sec.}}{\text{Pen. 77°F 100 g/5 sec.}} \qquad (3)$$

and

Susceptibility factor

$$= \frac{\text{Pen. 100°F 100 g/5 sec.}}{\text{Pen. 77°F 100 g/5 sec.}}. \qquad (4)$$

Eq. (3) is obviously a poor measure of susceptibility because the consistency is measured at three different unknown and changing stresses, and three different lengths of time. Eq. (4) compares consistency at different temperatures under unknown shearing stresses, which change at different rates. It cannot be used for comparing the susceptibility of bitumens of different consistencies because it is not a measure of the rate of change of consistency with temperature. In addition to the above criticisms, both Eqs. (3) and (4) are limited in application to asphalts harder than 70 to 75 penetration at 77°F 100 g/5 sec. With softer asphalts the penetrations at higher temperatures, using the prescribed loads, cannot be obtained.

Three other equations that have been suggested for calculating the susceptibility of asphalts should be mentioned:

Susceptibility factor[14]

$$= \frac{\text{Hardness at 32°F} - \text{Hardness at 115°F}}{\text{Softening Point °F (Kramer-Sarnow)}} \times 100 \qquad (5)$$

[5] C. U. Pittman and R. N. Traxler, Physics **5**, 221 (1934).
[6] H. Umstätter, Koll. Beihefte **39**, 265 (1934).
[7] K. A. Hoepfner and H. Metzger, Asphalt und Teer **30**, 258 (1930).
[8] K. A. Hoepfner, Tech. Gemeindeblat **32**, 177 (1929).
[9] "Wie prüft man Strassenbaustoffe?" Allgemeiner Industrie-Verlag G.m.b.H. Berlin (1932).
[10] H. Lenhard, Asphalt und Teer **34**, 254, 270 (1934).
[11] H. Lenhard, Asphalt und Teer **34**, 867 (1934).
[12] G. H. Klinkmann, Asphalt und Teer **35**, 530 (1935).
[13] Am. Soc. Testing Materials. Designation D-5-25. See also reference 16.
[14] H. Abraham, *Asphalts and Allied Substances*, third edition (D. Van Nostrand Co., Inc., New York, 1929), p. 672.

where hardness is defined "as the cube root of the number of grams which must be applied to a circular flat surface one square centimeter in area to cause it to displace the substance at a speed of one centimeter per minute."

Fluidity factor[15]

$$= (\text{Furol Vis. } 275°\text{F} - \text{Pen. } 77°\text{F } 100\text{ g}/5\text{ sec.})\,(\text{Pen } 77°\text{F } 100\text{ g}/5\text{ sec.})/100 \quad (6)$$

and

$$\text{Float test index}[16] = (\text{Float at } 176°\text{F} \times \text{Pen. } 77°\text{F } 100\text{ g}/5\text{ sec.})^{\frac{1}{4}}. \quad (7)$$

Eqs. (5), (6) and (7) do not measure change of consistency with temperature because they are arbitrary formulas for which one or more factors must be constant if different asphalts are to be compared.

In an effort to evaluate the susceptibility of asphalts to temperature, Holmes, Collins and Child[17] have set up three indices, two of which are analogous to that devised for lubricating oils.[18] For normal atmospheric temperatures these authors base their index upon the relationship between penetration and softening point expressed by the equation:

$$\log m = a \log P + \log K \quad (8)$$

or,

$$m = KP^a \quad (9)$$

where m is the Ring and Ball softening point,
P is the penetration, 77°F 100 g/5 sec.,
and a and K are constants.

An arbitrary index scale was established by using Mexican asphalt as the 100 point and petroleum tar obtained by cracking virgin gas oil under high temperature and pressure as the zero point on the scale. Iso-softening point lines were drawn from which the index of an asphalt of known penetration and softening point could be determined. This index is satisfactory as a measure of relative susceptibility but Eqs. (8) or (9) should be critically examined. A similar type of relationship has been found[1] not to correlate penetration and viscosity accurately.

To evaluate the susceptibility of bitumens in the lower temperature ranges, Holmes, Collins and Child propose the following:

$$\text{Susceptibility factor} = \frac{\text{Pen. } 77°\text{F } 100\text{ g}/5\text{ sec.}}{\text{Pen. } 32°\text{F } 200\text{ g}/60\text{ sec.}}. \quad (10)$$

This formula is subject to the same criticisms as Eq. (4) and in addition different loads are applied to the needle for different lengths of time at the two temperatures employed.

The third index, proposed for measuring susceptibility at elevated temperatures, employs Furol viscosity at 275°F and penetration at 77°F 100 g/5 sec. These characteristics were related in the same manner as were penetration and softening point in Eqs. (8) and (9). An index scale was again established employing Mexican asphalt as the 100 point and petroleum tar as the zero point. Since a simple expression, such as that proposed by Holmes, Collins and Child, does not accurately relate penetration and viscosity at low temperatures,[1] obviously a complex relationship also exists between penetration and Furol viscosity at 275°F.

Proposed Viscosity Index

From the above review of the various methods which have been proposed for comparing the susceptibilities of different asphalts, it appears that no simple and logical index has been developed because there has been no clear definition of the term susceptibility. However, if the meaning set forth at the beginning of this paper, i.e., the change of viscosity with temperature, is accepted, it follows that the expression for an index will be a function of the slope of some linear temperature-viscosity relation. The most simple index would be the slope of an arithmetical plot of temperature against viscosity but such a plot is not linear even over a very short temperature range. For the asphalts considered here, a plot of temperature against the logarithm of viscosity is essentially a straight line over a temperature

[15] J. Zapata, Proceedings of Assn. of Asphalt Paving Technologists, page 83, Jan. 30 (1935), Chicago, Ill.
[16] E. F. Kelley, Proceedings of Ass'n of Asphalt Paving Technologists, page 62, Jan. 30 (1935), Chicago, Ill.
[17] A. Holmes, J. O. Collins and W. C. Child, "Measuring the Susceptibility of Asphalts to Temperature Changes." Presented before Petroleum Division A. C. S., New York, April (1935).
[18] E. W. Dean and G. H. B. Davis, Chem. Met. Eng. **36**, 618 (1929).

range below the softening point (e.g., from about 15° to 35°C). Also, at temperatures well above the softening point (e.g., 80° to 120°C) data obtained[5] plot to be approximately a straight line.

On a semi-log plot, then

$$\log \eta = at + \log b, \tag{11}$$

where η is the viscosity in poises, t is the temperature (°C) and a and b are constants. For asphalts the value of a, the slope, is always negative.

Eq. (11) may be written

$$\eta = b\ 10^{at}. \tag{12}$$

The rate of change of viscosity with respect to temperature for this relation is a function of the slope a, since

$$d\eta/dt = a\eta_0 \log_e 10, \tag{13}$$

where η_0 is the viscosity at which the rate of change is determined.

Obviously, the rate of change of η with respect to t is of no value for a susceptibility index since it varies with the viscosity. However, by dividing both sides of Eq. (13) by η_0 we obtain the percentage rate of change which is constant:

$$d\eta/\eta_0 dt = a \log_e 10. \tag{14}$$

This equation could be used for an index of susceptibility but it would compare asphalts in units having no practical value since it involves infinitesimal changes in the variables.

It is comparatively easy, however, to derive an expression for evaluating the percentage change in viscosity for a definite interval in temperature. The percentage change in viscosity from t_1 to t_2 is given by the following equation:

$$\text{Percent change} = 100\left(\frac{\eta_2 - \eta_1}{\eta_1}\right) = 100\left(\frac{\eta_2}{\eta_1} - 1\right), \tag{15}$$

where η_1 and η_2 are the viscosities in poises at t_1 and t_2, respectively.

Percentage change is a function of the slope, since

$$a = \frac{\log \eta_2 - \log \eta_1}{t_2 - t_1} = \frac{\log (\eta_2/\eta_1)}{t_2 - t_1}, \tag{16}$$

then $$\log (\eta_2/\eta_1) = a(t_2 - t_1) \tag{17}$$

and $$\eta_2/\eta_1 = 10^{a(t_2 - t_1)}. \tag{18}$$

Therefore, Eq. (15) becomes:

$$\text{Percent change} = 100(10^{a(t_2 - t_1)} - 1). \tag{19}$$

This equation states that the percentage change in viscosity for a definite interval of temperature is constant over the temperature range for which Eq. (11) is valid. For asphalts, at any temperature, the percentage change in viscosity for an interval of temperature rise is smaller than for the same interval of temperature drop.

It is, therefore, proposed that the temperature susceptibility of an asphalt be measured by the percentage decrease in viscosity for 1°C rise in temperature over any range for which Eq. (11) applies. The numerical value for the index is then given by Eq. (19) wherein $(t_2 - t_1)$ is equal to 1. It is only necessary to know the viscosity of the asphalt at any two temperatures within the specified range; the asphalt viscosity index may then be expressed as:

$$\text{A.V.I.} = 100(10^a - 1)$$

$$= 100[(\eta_c/\eta_d)^{1/(t_c - t_d)} - 1], \tag{20}$$

where η_c and η_d are the viscosities, in poises, of the asphalt at temperatures t_c and t_d (°C), respectively. The values obtained for the A.V.I. are negative since the viscosity decreases with temperature, but from the definition proposed

TABLE I. *Identification of asphalts.**

Designation	Source (type)	Process	Penetration 32°F 200/60	Penetration 77°F 100/5	Penetration 115°F 50/5	Softening Point—°F R and B
A	Mexican	Batch steam	17	62	—	126
B	Venezuelan	"	18	61	282	126
C	Trinidad	"	—	60	—	118
D	Fluxed Refined Bermudez Lake Asphalt	—	16	61	298	122
E	Fluxed Refined Trinidad Lake Asphalt	—	16	62	300	125
F	Californian	Vacuum	5	35	244	122
G	Californian	"	6	55	soft	117
H	Mid-Continent	"	11	41	229	132
I	Mid-Continent	"	15	56	305	123
J	Mid-Continent	"	13	63	soft	124
K	Venezuelan	"	9	34	175	133
L	Venezuelan	"	12	57	324	124
M	Venezuelan	Batch steam	16	57	265	124
N	Mexican	Vacuum	17	55	272	126

* Asphalts *A* to *E* inclusive have been described previously.[5] Asphalts *K*, *L* and *M* were prepared from a mixture of heavy gravity with some medium gravity petroleum from the Mene Grande field in Venezuela.

TABLE II. *Viscosity-temperature data.*

TEMP. (°C)	VISCOSITY—(Poises × 10^{-6})													
	A	*B*	*C*	*D*	*E*	*F*	*G*	*H*	*I*	*J*	*K*	*L*	*M*	*N*
15	92.0	63.3	64.9	36.9	43.2	—	—	—	—	—	—	—	—	—
16	—	—	—	—	—	—	43.6	—	—	—	—	—	—	—
20	22.6	17.6	14.7	—	12.5	32.5	—	—	—	—	50.3	19.6	16.5	20.3
21	—	—	—	9.57	9.49	—	11.4	40.2	14.1	11.0	—	—	—	—
25	6.98	6.24	3.35	3.66	4.06	9.19	3.22	13.6	4.91	3.89	14.0	4.58	5.47	6.99
30	2.75	1.81	0.902	1.28	1.32	2.13	0.489	4.11	1.45	1.28	4.31	1.60	2.15	2.35
35	0.845	0.497	0.250	0.491	0.484	0.674	—	1.18	0.508	0.417	1.37	0.517	0.610	0.727

above their sign may be neglected. The A.V.I. has a definite meaning in that it evaluates the percentage change in the viscosity (in poises) of an asphalt for a one degree rise in temperature.

ASPHALTS USED

The fourteen different asphalts used in the present study are described in Table I as to source, method of preparation, penetration and softening point.

VISCOSITY OF ASPHALTS

The viscosities of the various asphalts were determined over the temperature range 15° to 35°C by means of the alternating stress method described by Bingham and Stephens.[19] The apparatus is simple and inexpensive, and is suitable for materials having viscosities above 10^6 poises. If data at higher temperatures are desired, or soft asphalts are to be investigated, the modified Bingham-Murray plastometer described elsewhere[5] may be employed. For consistencies above 10^5 poises the falling coaxial cylinder type of viscometer[20] may be used to advantage, while the rotating concentric cylinder type[21, 22] may be employed for a very wide range of consistencies.

The viscosities of the asphalts described in Table I are recorded in Table II.

Fig. 1 is a semi-log plot of the temperature-viscosity values in Table II for asphalts *A* and *C*. The curve for asphalt *C* illustrates how well the data in most cases may be expected to fit a straight line, whereas, the curve for asphalt *A* is given to show the least satisfactory approach of the experimental points to a straight line relationship. In the data given in Table II the accuracy in obtaining a straight line is probably limited chiefly by the accuracy with which the individual viscosities can be measured.

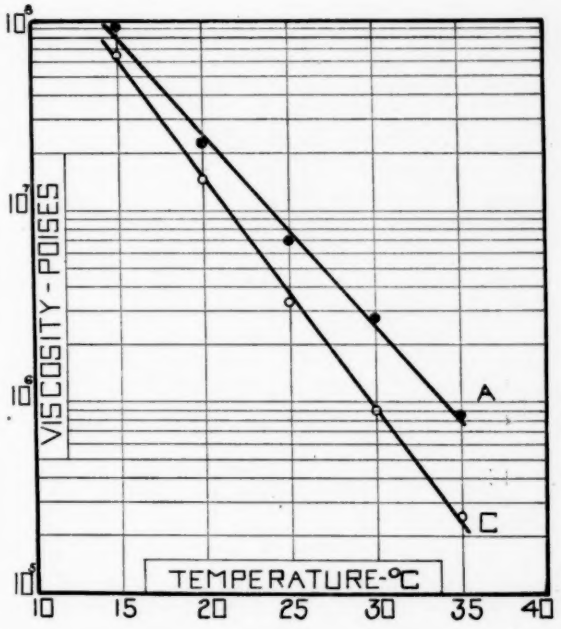

FIG. 1.

Although by using more complicated equations such as that proposed by Umstätter[6] it is possible to increase somewhat the temperature range over which a straight line relation is found to hold, it has not seemed necessary or advisable to use the more complicated expressions to obtain only a slightly greater range of applicability for the A.V.I.

[19] E. C. Bingham and R. A. Stephens, Physics **5**, 217 (1934).
[20] A. Pochettino, Nuovo cimento **8**, 77 (1914).
[21] M. Couette, Ann. chim. phys. (6) **21**, 433 (1890).
[22] M. Mooney and R. H. Ewart, Physics **5**, 350 (1934).

Discussion

The values of the A.V.I. for the fourteen asphalts described in Table I are listed in ascending order (increasing susceptibility to temperature) in Table III.

Table III. *Viscosity index of various asphalts.*

Asphalt	Source	a	A.V.I.
M	Venezuelan	−0.0925	19.2
N	Mexican	−0.0960	19.8
D	Bermudez Native Lake	−0.0966	19.9
E	Trinidad Native Lake	−0.0972	20.0
J	Mid-Continent	−0.0993	20.4
A	Mexican	−0.1004	20.6
L	Venezuelan	−0.1018	20.9
B	Venezuelan	−0.1019	20.9
I	Mid-Continent	−0.1027	21.1
K	Venezuelan	−0.1042	21.3
H	Mid-Continent	−0.1070	21.8
F	Californian	−0.1160	23.4
C	Trinidad Oil	−0.1224	24.6
G	Californian	−0.1231	24.7

Asphalts can probably all be classified under the three divisions proposed in Table IV.

Table IV. *Classification of asphalts based on susceptibility.*

A.V.I.	Classification
20.0 or below	Low susceptibility.
20.0 to 22.0	Intermediate susceptibility.
22.0 or above	High susceptibility.

Using this arbitrary classification we find that Mexican asphalt and fluxed refined Trinidad and Bermudez Lake asphalts show low susceptibility. Venezuelan and Mid-Continent oil asphalts are intermediate, while Californian and Trinidad oil asphalts are very susceptible.

Acknowledgment

The authors are indebted to Mr. C. E. Coombs for valuable aid in the development of the index, and to Mr. C. U. Pittman for criticisms and suggestions.

A Simplified Extrusion Plastometer for Unvulcanized Rubber

J. H. DILLON, *Physics Division, Research Laboratory, Firestone Tire and Rubber Co., Akron, Ohio*

(Received November 8, 1935)

A new extrusion plastometer for unvulcanized rubber is described. In this plastometer, the rubber sample is cut automatically and the extrusion chamber is filled in a single operation. The time of extrusion, which is measured by an accurate elapsed time indicator, is chosen as an index of plasticity. The plastometer is shown to be rugged, simple, and rapid in operation. Data are presented which establish the sensitivity and accuracy of the instrument. The results of the extrusion plastometer are discussed with respect to their correlation with those of the Williams plastometer and the United States Rubber Company shearing disk plastometer.

INTRODUCTION

AN extrusion plastometer operating at rates of shear comparable with those existing in rubber tubing machines has been described previously.[1] This plastometer was not designed to be a routine testing instrument but rather was intended for use in the determination of the value of a high speed extrusion test for the factory control of rubber stocks. The plastometer served satisfactorily in the capacity of a research instrument and has for some time been in constant use as a physical testing instrument where great rapidity of operation is not essential.

The results obtained with this plastometer were found to correlate with tubing machine behavior.[2] It was also found that the extrusion plastometer results agreed better with factory experience with various types of masticated gum rubber than did the Williams plastometer results.[3] It was learned by experience with the extrusion plastometer, when used as a physical testing instrument, that its results agreed closely with calender behavior.

In many cases, it was found that the extrusion plastometer results did not correlate with Williams plastometer results and that, in general, the extrusion plastometer appeared to be much more sensitive than the Williams plastometer.

The next step after establishing the value of the high speed extrusion test was to design an extrustion plastometer suitable for routine control testing. Such an instrument must be rugged in construction, rapid and simple in operation, and must yield precise results. The extrusion plastometer, which is described in this paper, was designed to fulfill these requirements and at the same time to give the same type of test results as those given by the original experimental plastometer.

DESCRIPTION OF THE EXTRUSION PLASTOMETER[4]

The new extrusion plastometer is illustrated in section in Fig. 1. The apparatus with which the extrusion is performed is shown at the right; the closing mechanism at the left. The two parts of the apparatus are linked together along line A–A.

The extrusion chamber consists of two members 3 and 4. The upper member 3 of the chamber has for its lower part a circular hardened steel knife edge 5 of diameter 7.62 cm (3 in.) fitting into a circular groove in the lower member 4. The hardened steel extrusion die 2 is threaded into the lower member. The die is essentially the same as that employed with the original plastometer[1] and is 3.18 mm (1/8 in.) in diameter and 4.77 mm (3/16 in.) in length. Cartridge-type electric heating elements are mounted symmetrically in holes 6 in both top and bottom members of the chamber. The Bakelite members 15 provide thermal insulation for the chamber. The extrusion is performed by a steel piston 1.88 cm (3/4 in.) in diameter which is actuated by a 17.8 cm (7 in.) air piston. The stroke of the piston is limited to 1.88 cm (3/4 in.) by a stop 27 and an adjustment screw 13. A turned ring 10 on the tail rod 9 actuates levers which make and break electrical contacts 11 and 12 at appropriate times just after the beginning and just before the end of the stroke, respectively. Thus, at the beginning of the stroke, contact 12 is closed and contact 11 is open. Just after the beginning of the stroke, 11

[1] Dillon and Johnston, Physics **4**, 225 (1933).
[2] Dillon and Torrance, Physics **6**, 53 (1935).
[3] Dillon, Ind. Eng. Chem. **26**, 345 (1934).

[4] The engineering design of the plastometer was made by Mr. R. W. Allen.

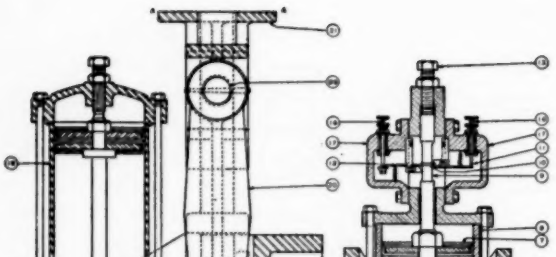

FIG. 1. Simplified extrusion plastometer.

is closed, completing the circuit with an elapsed time indicator which is accurate to within ±0.05 sec. The indicator runs until just before the end of the stroke when contact 12 is opened, breaking the circuit. The contact or housing members 17 are removable to permit adjustment of the contacts by means of screws 16.

The temperature of the extrusion chamber is maintained constant to within ±1°C by means of a bimetallic spiral regulator mounted in a hole in the lower member 4 of the cavity. The contacts of the regulator actuate an inductive relay which makes and breaks part of the heating current through the cartridge heater coils. The temperatures of both upper and lower members 3 and 4 are measured by means of mercury-in-glass thermometers inserted in closely fitting holes.

The lower member of the chamber 4 is movable vertically through a distance of 7.6 cm (3 in.) by means of the closing mechanism shown at the left of Fig. 1. The closing mechanism consists of a 17.8 cm (7 in.) air cylinder 18 pivoted at 22, a bell crank 19 and a toggle member 20. Downward motion of the air piston rotates the bell crank about pivot 23 and swings the lower end of the toggle to the left, thus lowering the lower member 4 of the chamber. Upward motion of the air piston closes the chamber. Because of the great mechanical advantage possessed by the air piston-toggle mechanism, the lower element 4 can be pressed against the upward element 3 with a force of 45,000 kg (50 tons) or more.

The plastometer is operated as follows. A slab of rubber stock taken from a mill and subsequently preheated to the testing temperature is folded once and placed on the lower member of the chamber 4. It is unnecessary to cut the slab to any particular size or shape except that it must be at least 1.88 cm (3/4 in.) in thickness and 7.6 cm (3 in.) square in the folded form. Air is admitted to the lower part of the air cylinder 18, thus activating the closing mechanism. As the member 4 is raised, the rubber is forced into the approximately hemispherical chamber, the excess extruding through the die 2. At the end of the closing operation, the chamber is completely filled with rubber. The air contained by the rubber either dissolves in the rubber or passes up past the extrusion piston 1 and out through the ducts 14. An interval of 15 to 40 seconds is required for the chamber to close, depending on the type of rubber stock used. The rubber is allowed to remain in the chamber for a short period to compensate for inaccuracies in the temperature of the preheating device. The interval between placing the rubber on the lower member 4 and starting the extrusion piston 1 is 2.5 minutes with the present method of preheating (air ovens).

At the end of this interval, air is admitted to the top of the cylinder 8, thus driving the piston 1 downward and extruding a definite volume of rubber (5.45 cm^3) through the die 2. The time required for the extrusion of this fixed volume is recorded by the elapsed time indicator and is taken as the plasticity index of the stock. The extrusion time varies from 2 to 60 seconds, depending on the type of stock being tested. An air pressure of 1.4 kg/cm^2 (20 $lbs./in.^2$) is used with soft stocks and 2.1 kg/cm^2 (30 $lbs./in.^2$) with tread stocks.

At the end of the extrusion, the chamber is opened. The rubber remaining in the chamber is removed and then the piston is raised. This last sequence of operations is quite important for, by removing the rubber from the chamber before raising the piston, sticking of rubber to piston and consequent clogging of the piston bearing are avoided. The rubber is removed from the upper part of the chamber by placing a piece of scrap rubber on the lower member 4, raising the lower member just to the point where the rubber in the upper member sticks to the piece of scrap rubber, again lowering 4 and removing the rubber from the upper member by pulling downward on the scrap rubber.

The method now employed for preheating the

rubber samples consists in placing the samples in electrically heated ovens at 3-minute intervals and removing them at the same rate. The capacity of the ovens is such that 8 samples can be heated at one time, i.e., each sample is preheated for 24 minutes. The temperatures of the ovens are maintained constant to within ±0.5°C by the use of bimetallic spiral regulators and efficient circulation of the air. Because of the variable thickness of the samples and the inefficiency inherent in the heat transfer from a gas to a poorly conducting solid, the temperatures of the samples are not as uniform as desired. Thus, as explained earlier, it is necessary to leave the samples 2.5 minutes in the plastometer chamber, so that the average total time of test is 3 minutes. With more efficient preheating, as would be furnished by a multiple platen press, the average time of test can be reduced to 1.5 minutes.[5]

Performance of the Extrusion Plastometer

The ruggedness of the simplified extrusion plastometer has been established by over two years of practically uninterrupted service. None of its parts have shown serious wear. In fact, the extrusion die, which was replaced after 2 years of service, was found to be enlarged only enough to cause a variation of less than ten percent in the results as compared with those obtained with the new die.

No difficulty with friction in either the extrusion piston or the air piston has been experienced since the instrument was first lined up. To avoid frictional difficulties, the edges of the cup leathers were shaved very thin and they were thoroughly soaked in neat's-foot oil. Measurements are made thrice daily of the time required for the piston to complete its downward stroke with the air pressure in the cylinder reduced to 0.28 kg/cm² (4 lbs./in.²) and with no rubber in the chamber. This time is 0.1 second or less with the plastometer at the testing temperature 77.8°C (172°F). Possible starting friction is eliminated as a source of error by allowing the piston to travel a short distance (1 mm) before starting the elapsed time recorder.

Error in the elapsed time indicator is less than ±0.05 second. It is simply a synchronous motor (1 r.p.s.) attached to a Veeder counter reading to 0.1 second. The fact that only one number is indicated by the device at the end of the extrusion practically eliminates human error of observation.

The matter of complete filling of the extrusion chamber has caused no trouble. In fact, rubber "biscuits" removed from the chamber either before or after extrusion are found to be entirely homogeneous. The fact that the chamber is filled completely is demonstrated by the uniformity of the extruded volume (see Table I).

The accuracy of the extrusion plastometer, with the samples preheated for 20 minutes in the extrusion chamber, is shown for three typical stocks in Table I. When the samples are preheated in the air ovens, the accuracy is somewhat less. However, even with inadequate preheating,

Table I. *Accuracy of extrusion plastometer.* Samples preheated in plastometer chamber 20 minutes at 77.8°C (172°F); driving pressure—172 kg/cm² (2460 lbs./in.²).

Stock	Extrusion Time (sec.)	Extruded Weight (g)	Range (%)	Mean Deviation (%)
Inner tube	1.8	5.14	11	±2.8
	1.9	5.31		
	1.7	5.24		
	1.8	5.21		
Mill massed smoked sheets	23.1	4.61	19	±2.7
	23.7	4.60		
	25.7	4.62		
	27.8	4.57		
Tread	10.5	5.77	4.8	±1.4
	10.4	5.77		
	10.1	5.82		
	10.6	5.79		

Table II. *Sensitivity of extrusion plastometer. Captax Skim Stock.*

Batch	Williams Plastometer (Y_3)	Extrusion Time (sec.)
1	2.87	8.7
2	2.53	8.9
3	2.58	10
4	2.71	14
5	3.00	15
6	3.00	20
7	3.25	30
8	3.45	52
9	2.98	55

Conditions of Test

Extrusion plastometer: 20-minute preheat at 80°C, 20 lbs./in.² air pressure.

Williams plastometer: Y_3 is the separation of the plates after a 3-minute compression at 85°C.

[5] Since this article was prepared, a method of preheating the rubber samples in a water-heated platen press has been developed and has been put into routine practice. With this method, the total time of test has been reduced to 1½ minutes and the accuracy of the test has been increased to a value equal to that given in Table I.

the selectivity[6] of the extrusion plastometer ranges from twice to twenty times that of the Williams plastometer when the two instruments correlate. When they fail to correlate, of course, the relative sensitivity of the two instruments has no meaning. The data of Table II give some indication of the manner in which the Williams plastometer and extrusion plastometer results compare on a regular factory skim stock.

Results

Data giving the relationships of the efflux rate *versus* driving pressure, temperature, etc., for the simplified extrusion plastometer, are omitted in this paper since these relationships are the same as those found for the original experimental extrusion plastometer.[1] It is interesting to note, however, the difference between the plasticity-*versus*-temperature curves obtained with the original experimental extrusion plastometer and those obtained with the United States Rubber Company shearing disk plastometer.[7] (See Fig. 2.) The data of Fig. 2 were obtained using the same batches of rubber in the two plastometers in each of the three cases; namely; unbroken (unmasticated) smoked sheets, mill-massed smoked sheets, and plasticated smoked sheets. For the case of unbroken rubber in the shearing disk plastometer, a negative temperature coefficient of plasticity was found in the higher temperature range, in agreement with the results of Mooney.[7] The other two curves for the shearing disk plastometer show very little change of plasticity with temperature. On the other hand, the results of the extrusion plastometer show a rapid increase of the plasticity index with increasing temperature in all cases. Furthermore, the results of the shearing plastometer indicate that the plasticated rubber (1 pass through the Gordon plasticator) is softer than the mill-massed rubber, whereas the extrusion plastometer indicates just the opposite conclusion. These discrepancies between the results of the two instruments may be explained in part by the fact that the extrusion plastometer operates at a much higher rate of shear than the shearing plastometer. Another reason for this disagreement is that a certain amount of slippage takes place in the die of the extrusion plastometer, whereas slippage is excluded in the shearing plastometer. A third reason for the disagreement may lie in the fact that the observations of the shearing disk plastometer are made at thixotropic equilibrium, whereas those of the extrusion plastometer probably are not.

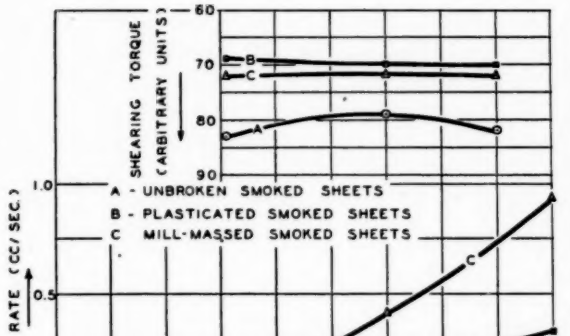

FIG. 2. Plasticity indices *vs.* temperature.

It should be noted that the two plastometers are designed on very different bases. The shearing disk plastometer is so constructed that a precise measurement of a fundamental physical property of rubber, the shearing viscosity, is obtained. The extrusion plastometer was built up with the idea of duplicating as accurately as possible the conditions existing in processing machines and gives a more or less empirical measure of the softness of rubber stocks under these conditions. Without discussing further the relative desirabilities of these distinct types of testing instruments, suffice it to say that it has been found that the results of the simplified extrusion plastometer are entirely reliable in mill room control work. The ruggedness of the extrusion plastometer as well as its reasonably short testing cycle are qualities which make it a practical instrument for the routine testing of the plasticity of rubber stocks.

Acknowledgment

In conclusion, the author desires to express his appreciation to N. Johnston, R. W. Allen, and G. Watt for their parts in the development of the extrusion plastometer described in this paper and to N. A. Shepard, under whose direction this work was performed.

[6] The "selectivity" is defined as the percentage difference between 2 observations on different stocks divided by the average maximum percentage error.

[7] Mooney, Ind. Eng. Chem., Analyt. Ed. **6**, 147 (1934).

Book Review

First Report on Viscosity and Plasticity. By J. M. BURGERS *et al.* Committee for the Study of Viscosity, Academy of Sciences of Amsterdam, 1935. Pp. 256+viii, roy. 800. Price 10 guilders, paper; 11 guilders, cloth.

Dr. G. E. Hale's suggestion to the International Council of Science that a committee be formed "for instruments and methods of research" brought this committee into existence. It considered that "the subject of viscous and plastic deformation seemed particularly well-suited to provide a theme that could bring together scientists from rather various domains of physics, chemistry and biology." The Committee consisted of Dr. H. R. Kruyt and Dr. H. G. Bungenberg de Jong for physical chemistry; Dr. W. H. Keesom, physics; Dr. F. M. Jaeger, chemistry and crystallography; Dr. C. J. van Nieuwenburg, industrial chemistry; Dr. J. M. Burgers, mechanical engineering; Dr. H. J. Jordan and Dr. W. A. Hijmans van den Bergh, biology and medicine.

They state that their objects were to gather and interrelate the information regarding viscous and plastic deformation, to make proposals regarding nomenclature, methods of measurement and their interpretation which would make possible the "unambiguous measurement of scientifically well-defined quantities." The present volume, because of the vastness of these problems, is largely restricted to the phenomenological aspect of the subject, but it is hoped to take up the problems of molecular and micellar structure in a further report.

The report is a vigorous and straightforward statement which will command attention from workers in this and many other fields. It is particularly pleasing to find interest rising in a field which has so long been neglected but has so multifarious applications, both industrial and scientific.

A liquid is defined as a substance which in the state of rest can support no other system of stresses than a hydrostatic pressure. Fluids may show elastic properties, but the term "liquids" is restricted to the cases where elastic properties, other than the ordinary compressional elasticity, are absent. This novel definition makes necessary the use of "liquidity" in place of *fluidity* in liquids. The term "differential liquidity" is used in place of mobility and distinguished clearly from the "mean liquidity," on p. 13.

The authors use the idea of the "yield value" which is defined, on p. 13, as the threshold value of the shearing stress τ, below which no appreciable shearing motion appears. They admit that it is sometimes rather difficult to state whether a definite yield value exists or not, and that if observations are sufficiently refined and times of observation duly extended, a flow may be detected for every value of τ. But in a great number of cases, considered from a practical view, a clearly apparent yield value can easily be distinguished. Later on, p. 125, van Bungenberg de Jong shows the necessity of properly constructed viscometers which have been carefully calibrated to determine very small yield values.

Van Nieuwenburg takes up the same question of yield value on pp. 166 *et seq.* and says, "As to whether in some cases a yield value is really present, it seems to me that this question has to be answered in the affirmative." He comes to what the reviewer regards as the correct conclusion, although differing from that of Burgers given above. "If as has been done, the yield value is defined as the value of the shearing stress, τ, where the asymptote intersects the τ-axis, and not at the beginning of the curved portion nothing else is done but what always (has) happened previously in experimental determinations. Moreover, such a definition permits us to leave aside the problem of whether a real yield value exists or not, which is the more desirable, as for technical applications it will hardly ever make any difference whether the diagram for small values of τ coincides with the τ-axis or deviates immeasurably little from it."

Van Nieuwenburg feels that various exponential formulas have focused attention on "the curved portion" of the flow curve, whereas this portion is rarely the most important part. He, therefore, p. 167, questions whether it is more than a mathematical "Spielerei." Nevertheless, he adopts, p. 168, the important conclusion due to Williamson that the flow curve is in fact hyperbolic with the formula $\tau=\eta D+fD/(a+D)$, which becomes Newton's formula when $f=0$ and the conventional formula of plastic flow when $a=0$.

The authors have devised a number of models with elastic springs and viscous elements to illustrate elastic and plastic deformation and the peculiar phenomena of the "after effect." These types of flow are also formulated mathematically. The chapter on the flow of crystalline substances is much needed. Many arguments are brought together in favor of the presence of regional structures of temporary character in liquids which possess a certain rigidity. They follow the theory of Andrade, but they point out that Andrade himself denied the existence of association in the first part of his paper, but later on in the same paper asserted that the temporary union which he postulated for the transfer of momentum resembles that involved in association. Therefore, they conclude that the process of shearing motion still remains somewhat vague.

The authors are not very hopeful of the result of the efforts being made to continue the use of "national" viscometers with viscosities expressed in centipoises or centistokes, because of the impracticability of conversion formulas. They prefer agreement upon a really suitable capillary viscometer and mention the Vogel-Ossag. The reviewer asks, perhaps naïvely, if there are absolute standards of viscosity and viscometers which are reliable, why is it necessary to specify viscometers any more than we do meter-sticks? If we do not have them, then obtaining should be the main point.

The question arises as to when are substances plastic? Since the stress at which the initial flow takes place, may depend in some instances upon the patience of the investigator, this is regarded as an undesirable criterion. van Nieuwenburg, p. 170, prefers to regard the flow of any material as plastic which is not definitely Newtonian.

There are practically no printer's errors and it is perhaps not surprising that so excellent linguists as the Dutch can write a book in a foreign tongue with scarcely a misuse of idiom. It is unfortunate that the book has no index, but this will doubtless be supplied in a later report.

EUGENE C. BINGHAM